▌Photosensitizers
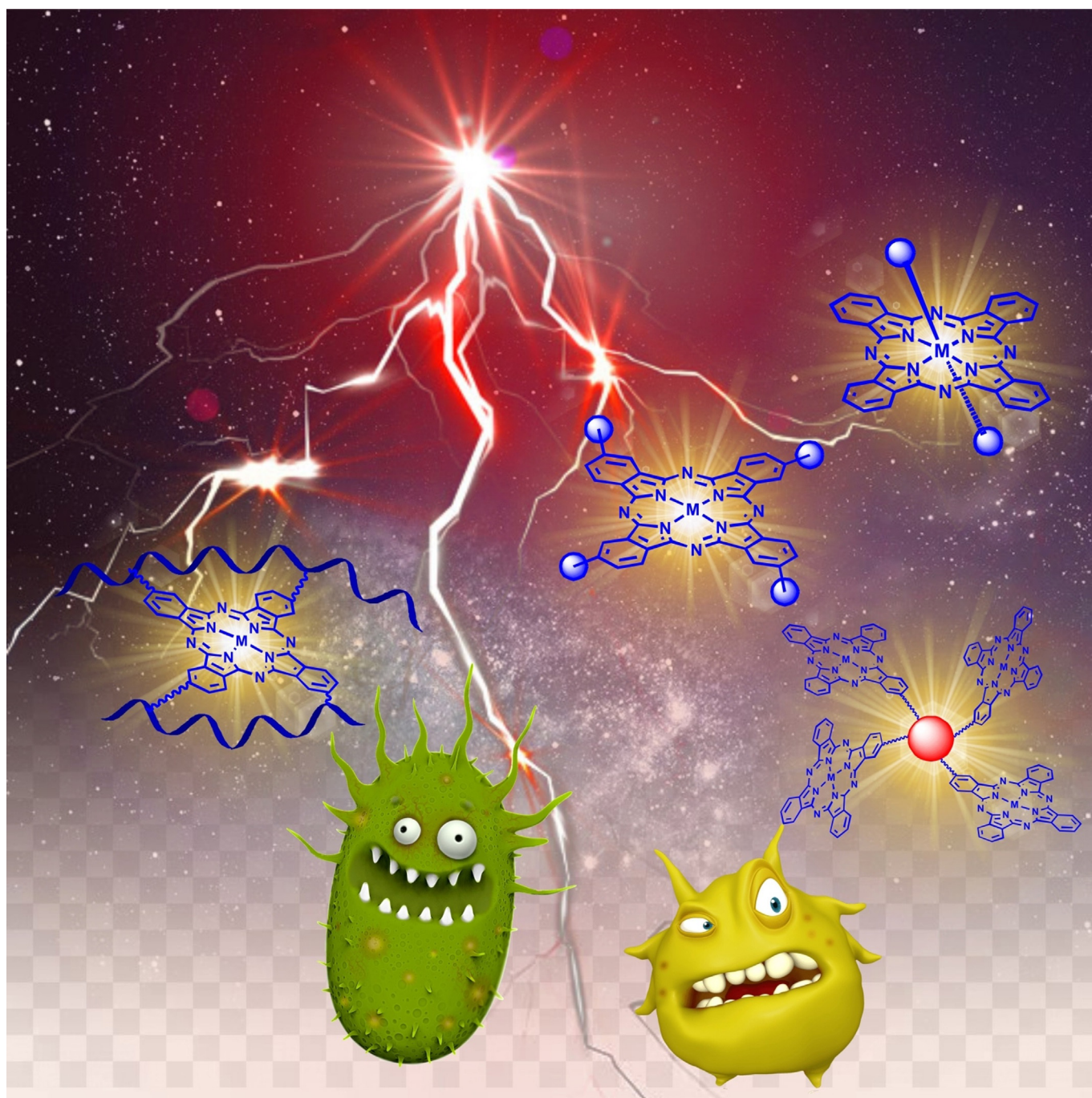
Turning Photons into Drugs: Phthalocyanine-Based Photosensitizers as Efficient Photoantimicrobials

Anzhela Galstyan*[a]

Chemistry–A European Journal

Review
doi.org/10.1002/chem.202002703

**Chemistry
Europe**
European Chemical
Societies Publishing

Abstract: One of the most promising alternatives for treating bacterial infections is antimicrobial photodynamic therapy (aPDT), making the synthesis and application of new photoactive compounds called photosensitizers (PS) a dynamic research field. In this regard, phthalocyanine (Pc) derivatives offer great opportunities due to their extraordinary light-harvesting and tunable electronic properties, structural versatility, and stability. This Review, rather than focusing on synthetic strategies, intends to overview current progress in the structural design strategies for Pcs that could achieve effective photoinactivation of microorganisms. In addition, the Review provides a concise look into the recent developments and applications of nanocarrier-based Pc delivery systems.

1. Introduction

In recent decades, light-mediated treatment of diverse diseases has received considerable attention in clinics due to the ability of light to initiate biologically important processes with specific spatiotemporal control without physically disturbing the (bio)molecules.[1] Photodynamic therapy (PDT) is a minimally invasive light-based approach mostly developed to treat neoplastic diseases.[2] Due to the emergence and spread of multidrug-resistant bacteria, PDT has attracted much attention since the mid-1990s as an alternative treatment for infections caused by resistant bacteria.[3] Nowadays, as the development of new antibiotics is not keeping up with the growing rate of resistant bacteria, aPDT is becoming increasingly attractive.[4,5] This modality offers a number of advantages, such as activity against resistant bacteria and their virulence factors, short treatment times, and a simple application, among others. The therapeutic principle of aPDT is based on the production of reactive oxygen species (ROS) under irradiation that can oxidize key cellular components leading to cell death. The fundamental processes are the following: light-driven transfer of a PS into an unstable excited singlet state can lead to emission of the secondary photon in the form of fluorescence or to the transfer of the PS into the excited triplet state via intersystem crossing; the PS activity largely depends on its capability in intersystem crossing.[6] From this state, PS can phosphoresce and/or generate ROS via two competing pathways—Type I and Type II. The Type I mechanism generates hydrogen peroxide (H_2O_2), the superoxide anion radical ($O_2^{\cdot-}$), or hydroxyl radicals ($OH^{\cdot}$); the Type II mechanism generates singlet oxygen ($^1O_2$).[7] ROS are non-specific and can damage DNA and proteins as well as disrupt membrane function.[8] Recently, Hamblin et al. highlighted a new mechanism, known as a Type III mechanism, which involves oxygen-independent photoinactivation (Figure 1).[9]

Initially discovered in the field of microbiology,[10] PDT was mainly used for treating malignant and non-malignant tumours; as such, PS structures were modified to reach and destroy neoplastic lesions. A detailed discussion of anticancer PDT based on phthalocyanines (Pcs) is beyond the scope of this article; however, interested readers are directed to an excellent review on the topic.[11] Nevertheless, the primary features of an ideal PS for use in PDT are sufficient ROS generation upon irradiation, negligible dark toxicity, good photostability, and biocompatibility. Furthermore, to be applicable in antimicrobial PDT, a PS should have a high affinity for microbial cells, a lower risk of inducing damage to host cells, and the ability to prevent bacterial re-growth after treatment.[12] Many of the PSs that fulfil these requirements have low extinction coefficients and absorb light in the UV region, which has low tissue penetration. In this regard, Pc derivatives are of great interest and can offer myriad advantages, such as high one-photon absorption coefficients in the red visible region resulting from the extended conjugated structure (660–720 nm, $\log \varepsilon > 5$), high quantum yield of ROS generation, high photostability, and ease of chemical and physical modifications.[13] Due to their relatively easy preparation from readily available precursors, such as phthalonitriles, phthalic acids, phthalimides, among others, Pc derivatives can be synthesized on a large scale at a relatively low cost. Many excellent reviews highlighting the state-of-the-art approaches for synthesizing Pc deriva-
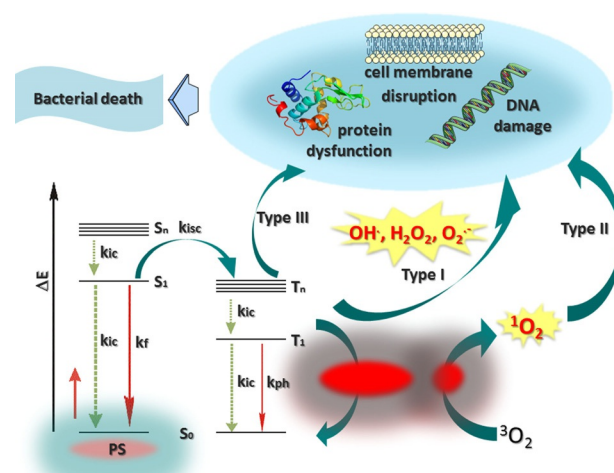
[a] *Dr. A. Galstyan*
Center for Soft Nanoscience, Westfälische Wilhelms-Universität Münster
Busso-Peus-Straße 10, 48149 Münster (Germany)
E-mail: anzhela.galstyan@wwu.de

The ORCID identification number for the author of this article can be found under: https://doi.org/10.1002/chem.202002703.

Figure 1. Simplified illustration of the Jablonski diagram showing the photophysical and photobiological processes involved in aPDT.

Chemistry–A European Journal

Review
doi.org/10.1002/chem.202002703

Chemistry Europe
European Chemical
Societies Publishing

tives and their analogues have previously been published.[14] Given these benefits Pc derivatives are the most promising PSs for aPDT applications. Thus, the scope of this Review focuses on Pc-based PSs and nanostructures that have been used in aPDT. In the following sections, I describe the functionalization strategies that enhance the photobiological activity of Pcs and highlight the current challenges and perspectives in this research area.

2. Structural Design Features

The most common modifications to the Pc macrocycle include introducing water-solubilizing groups, improving optical properties, attaching targeting units to ensure accumulation in bacterial cells, and prolonging the therapeutic function. Diverse pathways for synthesizing Pc derivatives and modifying their photophysical and photobiological properties have been systematically investigated over the last decades.[15] The Pc macrocycle can be substituted on the peripheral and/or non-peripheral position, and, depending on the metal centre, substituents can also be introduced into the axial positions.

PSs are thought to preferentially accumulate in actively dividing cells; hence, microorganisms that grow much faster than cancer cells should be sensitive to many PSs that are active against cancer. However, many studies have shown that the phototherapeutic effects of PSs against bacterial species depend on different PS characteristics. While the general mechanisms of photosensitized oxidation are the same, bacterial cells may not adequately bind and take up the PS. The bacterial membrane can efficiently protect bacteria from the PS, and, because of the limited diffusion range of toxic ROS, many known PSs become inactive or show low activity against microorganisms. Thus, structural modifications have been introduced to improve bacterial binding and uptake of PS. Even so, Gram-positive and Gram-negative bacteria have fundamental differences in susceptibility towards PSs due to differences in their cell wall composition. Gram-positive bacteria have thick (15–80 nm) but porous cell walls mainly composed of peptidoglycans,[16] such that non-cationic PSs can be taken up and can efficiently inactivate them. In contrast, Gram-negative bacteria contain a thin peptidoglycan layer surrounded by an outer membrane, and negatively charged lipopolysaccharides (LPS) are a major component of the cell wall.[17] Thus, PSs that possess intrinsic cationic charges are electrostatically attracted to the negatively charged cell envelope and can effectively bind to cell sites that are important for the cellular stability and/or cell metabolism. When this occurs, photoinduced generation of ROS can efficiently inactivate the cells.

In addition to the cationic vs. non-cationic nature of the PS, the nature of the metal centre also plays a role in inactivating bacteria. Due to their long-lived triplet states and efficient ROS generation, Zn^{II}, Si^{IV}, and Al^{III} Pcs are the most widely used Pc-based systems. SiPcs and AlPcs can additionally be substituted in the axial position to reduce the aggregation and increase the solubility of the PS, which are important properties for high photodynamic efficacy. Thus, the following section will discuss small molecule PSs and nanostructures containing different Pcs.

3. Molecular Photosensitizers

3.1. Silicon(IV)phthalocyanines

One of the most representative examples of a molecular Pc-based PS is the silicon(IV)phthalocyanine Pc4 (**1**, Figure 2) developed by Kenney et al. This molecule showed very promising therapeutic efficacy against different tumour cells,[18] cutaneous T cell lymphoma and psoriasis. Pc4 was also used for sterilization of blood components by V.I. Technologies (Vitex, Melville, NY, USA). In 2015, Baron and co-workers reported that Pc4 can be taken up by multiple strains of Gram-positive *S. aureus* (ATCC 25923, ATCC 43300, PFGE type 300) and disrupt the overall metabolic activity of the bacteria upon irradiation.[19] In particular, they showed that incubating 1 μM Pc4 with different *S. aureus* strains for 3 h at 37 °C followed by red light irradiation at 2 J cm^{-2} can lead to an almost complete elimination of bacteria. Among studied SiPcs, differently axially substituted derivatives have also been reported to be effective against bacteria. Synthesis of four SiPcs axially substituted with methylparaben, ethylparaben, propylparaben, and butylparaben, respectively (**2a** to **2d**), was achieved by nucleophilic displacement of two chloride substituents from SiPc(Cl)$_2$.[20] All these phthalocyanines showed similar fluorescence emission spectra in DMF and similar singlet oxygen quantum yields (≈ 0.47); the increase of the hydrocarbon chain from **2a** to **2d** did not show any quenching effect on singlet oxygen generation. In vitro studies performed with the Gram-positive cariogenic bacteria *S. mutans* surprisingly indicate that only **2c** has significant photoinactivation (> 3 log$_{10}$ reduction) at the applied concentrations (5 μM and 10 μM). However, the activity of **2c** against 48-h biofilms was very low, even at the highest concentration (10 μM) and a prolonged incubation time (1.5 h). The SiPc axially substituted with the group {4-[(1*E*)-3-oxo-3-(2-thienyl)prop-1-en-1-yl]phenoxy} (**3**, $\Phi_\Delta = 0.11$) showed, at a concentration of 64 μg mL^{-1}, a potent bactericidal effect against *S. aureus* and

Anzhela Galstyan studied chemistry at Yerevan State University and University of Siegen and obtained her PhD in 2010 form the Faculty of Chemistry and Chemical Biology at Technical University of Dortmund and International Max-Planck Research School in Chemical and Molecular Biology under the supervision of Prof. Dr. Bernhard Lippert. Then she moved to the Center for Nanotechnology, University of Münster for postdoctoral research in the group of Prof. Luisa De Cola (2011–2012). Following postdoctoral stay in the European Institute for Molecular Imaging, University Hospital Münster (2013–2016), she started her independent research in the Center for Soft Nanoscience, University of Münster in 2016. Her current research interests focus on the synthesis, self-assembly, nanotechnological and biological applications of phthalocyanines and related macrocycles.
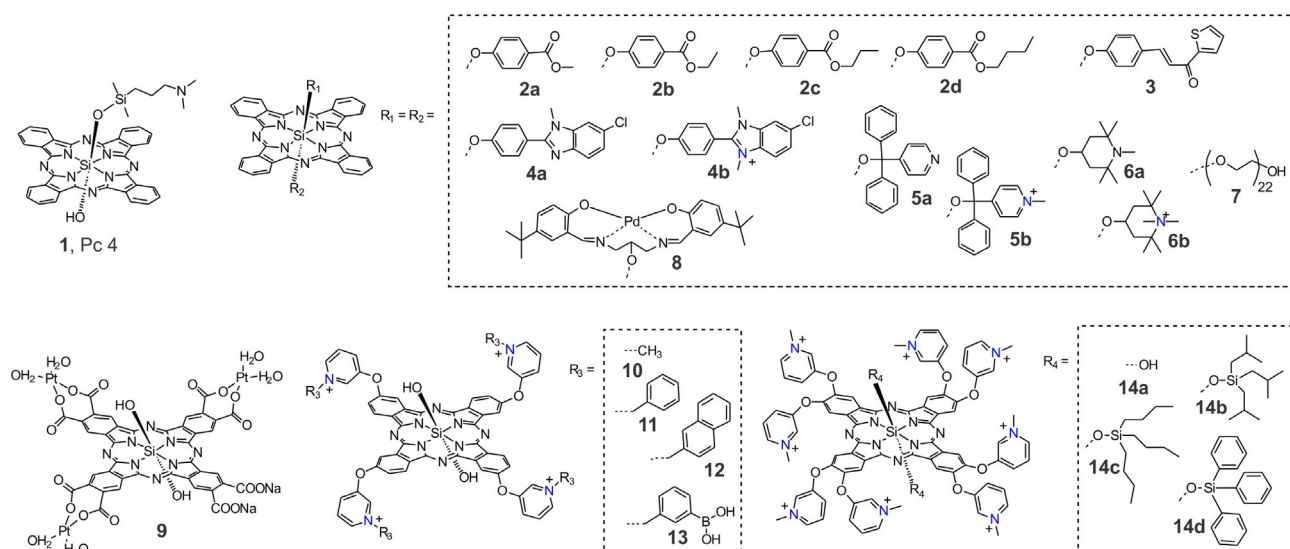
Figure 2. Chemical structures of some SiPc-based photosensitizers used in aPDT.

E. coli after irradiation with a light dose of 30 J cm^{-2}.[21] The same substitution pattern was used to decorate SiPcs with benzimidazole moieties (**4a**), which were further quaternized to produce a positively charged PS (**4b**).[22] As a result of photoinduced electron transfer between the phthalocyanine ring and axial ligands, the non-quaternized derivative **4a** showed $\Phi_\Delta = 0.42$, which is lower than that of the quaternized derivative **4b**, at $\Phi_\Delta = 0.69$. As expected, the cationic compound **4b** displayed a higher potency, with a 2.61 log$_{10}$ reduction, against *S. aureus* than did the neutral derivative **4a**, which had a 1.65 log$_{10}$ reduction.[23] An increase of the φ_Δ value from 0.15 to 0.33 was also determined for the axially substituted di-(α,α-diphenyl-4-pyridylmethoxy) silicon(IV) phthalocyanine (**5a**) and its quaternized derivative (**5b**). However, in this case, the neutral derivative **5a** showed a lack of efficacy, and **5b** was efficient only against Gram-positive *S. mutans* and *S. aureus*, showing full inactivation with a 10 μM solution at a light dose 50 J cm^{-2}.

For Gram-negative *P. aeruginosa*, the effect was negligible for concentrations up to 22 μM of **5b** and a light dose 100 J cm^{-2}. The same strategy was used to coordinate (1,2,2,6,6- pentamethyl-4-piperidinol) into the axial positions of the SiPc **6a** ($\Phi_\Delta = 0.31$ in DMSO), which was further quaternized to yield the water-soluble derivative **6b** ($\Phi_\Delta = 0.18$ in DMSO and $\Phi_\Delta = 0.15$ in phosphate-buffered saline).[24] Compared to **5b**, a lower concentration of **6b** (3–5 μM) was required to inactivate Gram-positive *S. mutans* and *S. aureus*. Even high concentrations of **6b** did not inactivate *P. aeruginosa*.

To confer hydrophilicity to SiPc, Uslan et al. used poly(ethylene glycol) in which there were 44 total O-CH$_2$-CH$_2$ units (**7**, $\Phi_\Delta = 0.49$ in DMSO and $\Phi_\Delta = 0.19$ in H$_2$O).[25] Incubating *E. coli* with 1000 mg mL^{-1} and 2500 mg mL^{-1} of **7** for 48 h in the dark reduced its viability by ≈90%, most likely due to the amphiphilic character of **7**.

To combine the photodynamic activity of Pc and the cytotoxic effect of Pd and Pt complexes, SiPc derivatives bearing an axial palladium(II)–Schiff base complex (**8**)[26] and a peripheral tris(diaquaplatinum)octacarboxy groups (**9**)[27] were synthesized, and their photophysical and antimicrobial properties were studied. When compared with the unsubstituted SiPcCl$_2$, the singlet oxygen quantum yield of **8** measured in DMSO increased from 0.18 to 0.47. The results of the photodynamic antimicrobial effect against *S. aureus* demonstrated that compound **8** possesses excellent photodynamic activity with a 3.26 log$_{10}$ reduction after 120 min irradiation, but it also showed dark cytotoxicity over the same amount of time. Due to the heavy atom effect, a significant improvement in the singlet oxygen quantum yield was also observed for complex **9** ($\Phi_\Delta = 0.58$) compared to a Pt-free derivative ($\Phi_\Delta = 0.26$). The antimicrobial photoinhibition studies on **9** showed that it inhibited *E. coli* in the dark and upon irradiation: The minimum inhibitory concentration required to inhibit the growth of 50% of organisms (MIC$_{50}$) was found to be < 8 × 10–4 mg mL^{-1} under illumination for 60 min.

To increase the activity of SiPcs, positive charges have been introduced into the peripheral positions of the tetra- or octa-*N*-methylpyridyloxy-substituted macrocycle. A comprehensive study done by our group determined the impact of lipophilicity and host-guest complexation on the molecular features of 2(3),9(10),16(17),23(24)-tetrakis(3-pyridyloxy) phthalocyaninato dihydroxy-silicon(IV) and its aPDT efficacy.[28] We showed that quaternized derivatives bearing methyl (**10**), phenyl (**11**), and naphthyl (**12**) substituents have similar singlet oxygen quantum yields ($\Phi_\Delta = 0.52$–0.56 in DMF and $\Phi_\Delta = 0.17$–0.25 in H$_2$O). However, the introduction of lipophilic groups enhanced the affinity of the PSs for bacteria and increased their photocytotoxic effect. Whereas there was a non-significant decrease of viable *E. coli* cells treated with a 1 μM solution of **10** and irradiated with red light (36 J cm^{-2}), compounds **11** and **12** achieved > 5 log reductions under the same conditions. To emphasize

Chemistry–A European Journal

Review
doi.org/10.1002/chem.202002703

Chemistry Europe
European Chemical
Societies Publishing

the role of hydrophilic moiety, we assessed the host-guest interaction between either phenyl- and naphthyl-functionalized silicon(IV)phthalocyanine and cucurbit[7]uril. The supramolecular structures showed significantly reduced activity most likely due to the decrease in lipophilicity (Figure 3).

Nevertheless, an increase of hydrophobicity is not always correlated with aPDT efficacy. The Torres group synthesized octa-cationic silicon (IV) phthalocyanine derivatives bearing eight N-methylated pyridyloxy substituents in their periphery and bearing either hydroxyl (**14a**) or different silyl ether moieties (OSi(iBu)$_3$, **14b**; OSi(nBu)$_3$, **14c**; and OSiPh$_3$, **14d**) at axial positions, and then they evaluated how the different axial and peripheral substituents influenced these SiPcs's spectroscopic, photochemical, photophysical, and biological properties.[29] For non-quaternized derivatives, an increase of ROS production from 0.32 to ca. 0.50 was observed upon the introduction of silyl ether moieties. From inactivation studies using a PS concentration of 20 μM and a light dose of 540 J cm^{-2}, results showed that the SiPc bearing an axial OH group was more efficient against Gram-positive *S. aureus* strains ($>99.99\%$) than were the SiPcs bearing different bulky silyl moieties. Inactivation of Gram-negative *E. coli* was not successful, even with **14a**.

In recent years, SiPc derivatives with targeted specificity have been designed and synthesized. Since extracellular polysaccharides known as bacterial glycocalyx are a major structural component of the bacterial cell surface (up to 75% of the surface) and contribute to the bacterial cell structural integrity, our group synthesized boronic acid-functionalized SiPc **13** to promote binding of PS to the bacterial cell surface; we then used this compound for photoinactivation of urinary tract-related *E. coli* isolates.[30] Although **13** generated similar amounts of ROS as previously reported SiPc derivatives ($\Phi_\Delta = 0.51$ in DMF and $\Phi_\Delta = 0.18$ in H$_2$O), we were able to significantly reduce bacterial cell viability (>5 log reduction, 36 J cm^{-2}) without causing excessive damage to the host tissue. Moreover, boronic acid-diol binding interactions allow PS to bind to

the biofilm matrix and to disperse it upon irradiation (Figure 4a).

The discovery that bacteria show specificities for binding carbohydrates has opened a new area for designing and synthesizing targeted agents. For instance, maltohexaose-based probes have been shown to bind to prokaryotes with high sensitivity using a bacteria-specific maltodextrin transport pathway. We recently showed that the maltohexaose-functionalized SiPc **15** labelled both Gram-positive and Gram-negative bacteria but selectively inactivated only the Gram-positive *S. aureus*.[31] In contrast, the mannose-conjugated photoprobe only labelled and killed the Gram-positive strain (>5 log$_{10}$ reduction, 36 J cm^{-2}). Flow cytometry measurements showed 30-fold increase in the binding affinity of the maltohexaose derivative compared to mannose functionalized SiPc. Nevertheless, absence of the activity towards the Gram-negative strain suggests that the maltohexaose-conjugated SiPc most likely sticks on the outer membrane of the bacteria and cannot diffuse towards the inner membrane. Thus, irradiation could not cause significant damage to the bacterial membrane and the bacteria remained viable (Figure 4b).

Since microbial cells show higher surface electronegativity than mammalian cells, amino-modified compounds have stronger binding ability to microorganisms. Due to its strong basicity and easy protonation, guanidine groups have often been introduced into antibacterial drugs to improve their interaction with target cells. Recently, the Huang group synthesized and characterized tri-arginine oligopeptide-containing SiPc (**16**, Figure 5).[32] The photophysical characteristics and biological activities were compared with its precursor and analogues containing mono- and tri-arginine oligopeptides. Results showed that an increase in the number of arginine on the substituents
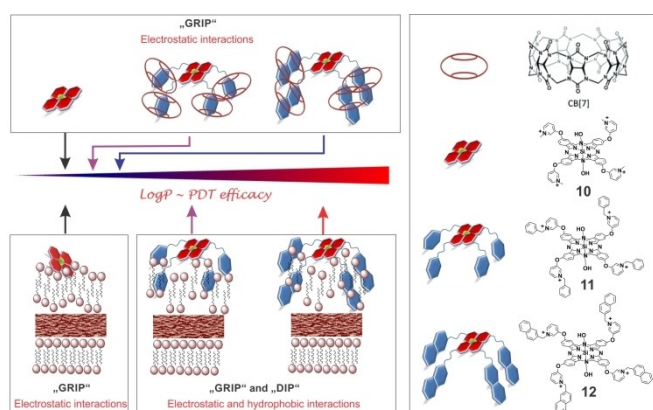

Figure 3. Schematic representation of change of lipophilicity upon host-guest complexation and probable dispositions of the compounds **10**, **11**, and **12** in the outer membrane of Gram-negative bacteria. Reproduced with permission from Ref. [28]. Copyright 2018, Wiley-VCH.
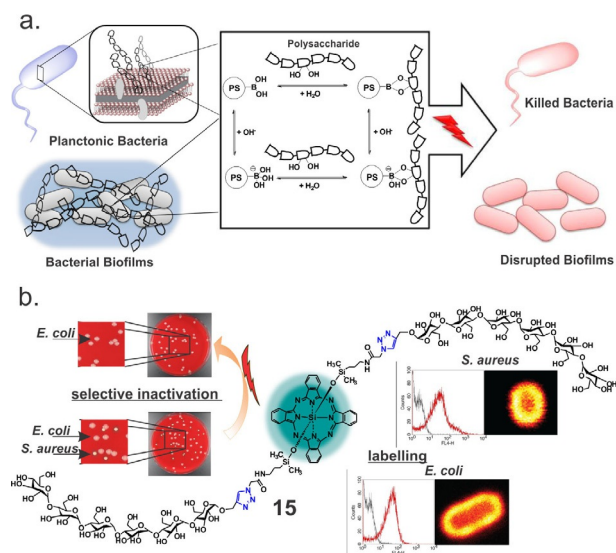

Figure 4. (a) The interaction between the photosensitizer **11** and polysaccharides of the bacterial cell membrane and the biofilm matrix. Reproduced with permission from Ref. [30]. Copyright 2017, Wiley-VCH. (b) Maltohexaose-conjugated silicon(IV)phthalocyanine for labelling and inactivation of bacteria. Reproduced with permission from Ref. [31]. Copyright 2016, Wiley-VCH.
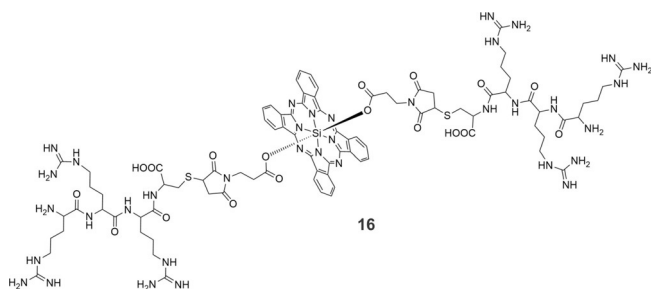
Chemistry–A European Journal

Review
doi.org/10.1002/chem.202002703

Chemistry Europe
European Chemical
Societies Publishing

Figure 5. Structure of tri-arginine oligopeptide-containing SiPcs **16**.

enhanced the Pc's ability to generate ROS and take up by bacteria, increasing overall aPDT effect. The IC_{90} values of **16** were calculated to be 0.3 μM against *S. aureus* and 0.6 μM against *E. coli*. *In vivo* studies on infected mouse model showed that *S. aureus* colonies could hardly be observed for the PDT-treated group, with an inhibition rate of 97.6%, while control groups showed unaffected *S. aureus* communities.

3.2. Zinc(II)phthalocyanines

Perhaps the most developed Pc-based PSs are those containing zinc(II) as a central metal, due to the ease of synthesis and possibility of obtaining low-symmetry derivatives with an optimal set of properties. Some ZnPc derivatives, such as CGP55847, photocyanine, and RLP068/Cl are currently in clinical trials. Among them, tetra-cationic RLP068/Cl (**17**) is a well-studied PS against localized infection.[33] In 2013, the Hamblin group studied the effect of RLP068/Cl on bacterial inactivation and wound healing in a mouse skin abrasion model using bioluminescent methicillin-resistant *S. aureus*.[34] The authors showed that the loss of colony forming units (CFU) closely paralleled the loss of bioluminescence, and total killing was achieved at 100 nM and at 5 J cm^{-2}. In an in vivo model, the luminescence intensity of scratched wounds inoculated with 10^8 CFU of methicillin-resistant *Staphylococcus aureus* (MRSA) was used to define the dose-response relationship of aPDT with RLP068/Cl. Similar to a previously published study,[35] treatment with RLP068/Cl led to significant bacterial inactivation and improvement in wound healing using 75 μM of the PS and 84 J cm^{-2} light at 690 nm.

A ZnPc derivative, peripherally substituted with four bis(N,N,N-trimethyl)amino-2-propyloxy groups (**18**), has been shown to be an efficient PS with a quantum yield of 0.54 for ROS generation in neat water, which is reduced to about 0.32 in phosphate-buffered saline.[36] Irradiation of *S. aureus* and *E. coli* cells incubated with 1 μM of **18** for 5 min with 675 nm light caused a 4 log$_{10}$ decrease in the survival of both strains. However, a large difference in photosensitivity was observed when the *E. coli* cells were irradiated after three washing steps; only a ≈2 log$_{10}$ decrease in survival was observed after 5 min irradiation. Electrophoretic analyses indicated that several proteins in the outer wall of photo-treated *E. coli* cells were the target of the initial stages of the irradiation, as shown by the disappearance of protein bands after 15 s of irradiation. These changes made the *E. coli* cell walls more permeable such that the PS could reach the cytoplasmic membrane, decreasing the activity of typical membrane enzymes.

Similar to studies described above, the Wang group synthesized amino group-substituted tetra-(**19a**) and octa-cationic (**19b**) phthalocyanines and tested their photophysical and light-mediated antimicrobial effects against *E. coli* in both a planktonic and biofilm state.[37] Both PSs were rapidly absorbed by the cells and had very good antimicrobial activity. For octa-cationic **19b**, smaller drug concentrations and light doses were needed to inactivate *E. coli* as compared with tetra-cationic **19a**. For instance, at a light dose 50 J cm^{-2} combined with **19a** at 20 μM, a nearly 3.1 log$_{10}$ reduction of *E. coli* was achieved, while **19b** showed nearly a 5 log$_{10}$ reduction at 30 J cm^{-2} light doses. For *S. aureus*, they showed that **19a** was more effective at inhibiting *S. aureus* growth at 24 J cm^{-2}, producing a 5.9 log$_{10}$ reduction, than **19b**, which produced a 4.8 log$_{10}$ reduction.[38]

To study the effect of hydrophilic-hydrophobic balance on the aPDT activity of ZnPcs, Kussovski et al. synthesized tetra alkyl-substituted cationic phthalocyanines with different hydrocarbon chains attached to the pyridyloxy group (**20a–d**).[39] The uptake studies showed a slight increase of binding from hydrophilic to more hydrophobic Pc complexes. Gram-negative *A. hydrophila* was used for the biological studies and was fully inactivated with **20a** (treated with 2.0 μM at a fluence rate of 60 mW cm^{-2}). The bacteria treated with **20b** had a <2 log$_{10}$ reduction for all drug concentrations. Complete photoinactivation at 3.25 μM for **20c** and 1.37 μM for **20b** was observed (Figure 6).

The same question was addressed by the Dąbrowski group. They synthesized a new family of cationic tetra-imidazolyl Pcs with a different number of positive charges and cationizing alkyl chains of different lengths (**21a–d**).[40] All ZnPcs were found to have high singlet oxygen quantum yields (0.66 < Φ_Δ < 0.72). Although the long alkyl chains in the cationic phthalocyanine **21b** led to significantly higher uptake by Gram-positive (*E. faecalis* and *S. aureus*) and Gram-negative (*E. coli* and *P. aeruginosa*) bacteria, reduction at 100 nM PS and a light dose of 10 J cm^{-2}), while **21c** was more active against Gram-positive species (>3 log$_{10}$ reduction) under the same conditions. Overall, **21a** might allow for effective aPDT for topical infections because of its low toxicity towards human keratinocytes (HaCaT cell line).

Recently Mantareva et al. studied aPDT efficacy of zwitterionic ZnPcs obtained by quaternization of the corresponding tetra- and octapyridyl-substituted Pcs with propanesulfonic acid.[41] Despite relatively high uptake and sufficient distribution of peripherally tetra-substituted ZnPcs (e.g., **22**) in pathogenic bacteria *E. faecalis* and *P. aeruginosa*, aPDT activity was low. Only ZnPc containing eight propanesulfonic substituents showed relatively high photoinactivation for both bacterial strains (>6 log$_{10}$ reductions, 6 μM PS, 50 J cm^{-2}) with minimal phototoxicity toward Balb/c 3T3 cells.

A series of structurally identical PSs with variable positive charges $n = 0, 4, 8, 12$ (**23**) were synthesized by Zhang et al and their activity against Gram-positive (*S. aureus*) and Gram-negative (*E. coli*) bacteria were investigated.[42] Interestingly,
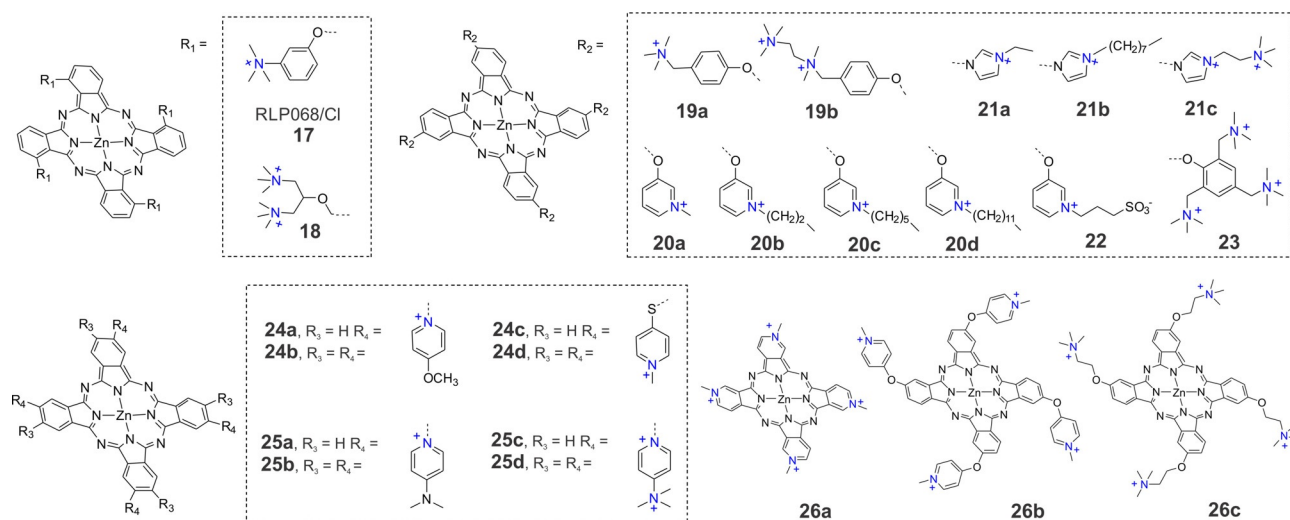
Chemistry–A European Journal

Review
doi.org/10.1002/chem.202002703

Chemistry
Europe
European Chemical
Societies Publishing

Figure 6. Chemical structures of some SiPc-based photosensitizers used in aPDT.

compound **23** with $n = 12+$ exhibited the highest amount of binding to bacteria, but structurally related ZnPc with $n = 8+$ turned out to have the strongest antibacterial effect among these compounds, with an IC_{50} value of 59 nM towards *E. coli* and 131 nM towards *S. aureus* at a light dosage of 5 J cm^{-2}. The authors also showed that ZnPc with $12+$ charges generated ROS primarily via the Type I mechanism, while ZnPc $4+$ and $8+$ created ROS by both the Type I and Type II mechanisms.

ZnPc derivatives containing trimethylammonium groups with a varied number and nature of the groups at peripheral positions were described by the Tomé group.[43] The photosensitizing potential of these compounds against a recombinant bioluminescent *E. coli* strain was shown to be dependent on the nature of the neighbouring group. For example, ammonium ZnPcs with eight charges or containing halogen atoms such as chlorine caused 4.9 and 5.6 log$_{10}$ reductions, respectively, with red light and 0 and 2.3 log$_{10}$ reductions, respectively, with white light (20 μM PS, 150 mW cm^{-2}, 30 min). The ammonium ZnPc derivative with fluorine as a neighbouring group failed to generate ROS and inactivate bacteria, which shows that simply increasing the number of positive charges does not necessarily increase the aPDT efficacy of a PS. The Tomé group also described an easy synthetic approach to obtain water-soluble inverted tetra- and octa-methoxypyridinium phthalocyanines (**24a** and **24b**) and compared their efficiency to photo-inactivate a recombinant bioluminescent strain of *E. coli* to that of thiopyridinium-substituted ZnPc (**24c** and **24d**).[44] Thus, they evaluated the effect of substitution pattern on PS photosensitization efficacy.[45] Upon irradiation with white light, **24b–d** caused significantly higher inactivation (2.8, 2.3, and 2.7 log$_{10}$ reductions) than **24a** (0.8 log$_{10}$ reduction), after 20 min of irradiation. When red light (620–750 nm) was used, the activity of **24a** was the lowest (0.9 log$_{10}$ reduction) followed by **24d** (2.3 log$_{10}$ reduction). The inactivation profiles of octa-substituted **24b** and tetra-substituted **24c** were higher (3.5 log$_{10}$ and 4.1 log$_{10}$ reductions, respectively).

Overall, this study highlighted that the position of the positive charge and the flexibility of the ligand influence the aPDT efficiency of the PS.

Later, the same group showed that the inactivation efficiency of ZnPcs containing inverted pyridinium groups can be enhanced by increasing the number and distribution of positive charges.[46] Differently charged ZnPc derivatives (**25a–d**) bearing dimethylaminopyridinium and their quaternized derivatives on the macrocycle periphery were synthesized and characterized. Under white-light irradiation, the aPDT response of all ZnPcs was very low, but under red light, the efficiency of **25c** and **25d** was strongly improved, resulting in an approximately 5.0 log$_{10}$ reduction in the bioluminescence of *E. coli* after a total light dose of 270 J cm^{-2}. No significant improvement was observed in the efficiency of **25a** and **25b** under red light. The authors noted that the activity of the PS was increased when the positive charges are suitably positioned to increase binding to the cell wall of Gram-negative bacteria.

Durantini and co-workers further explored the influence of substituents' photophysical and biological properties through a comparative study of three tetra-cationic ZnPcs.[47] In **26a** the charges are located directly over the phthalocyanine macrocycle, while in **26b** and **26c** the cationic centres are separated from the conjugated ring by an ether bond. All these PSs presented a high efficiency in the quantum yield of ROS production ($0.47 < \Phi_\Delta < 0.59$) in DMF, but the viability of microbial cells after a photodynamic inactivation experiment was different for each compound. Photosensitized inactivation of *E. coli* cellular suspensions decreased in the order of $\mathbf{26b} > \mathbf{26c} > \mathbf{26a}$. In particular, **26b** exhibited photosensitizing activity that caused a 4.5 log$_{10}$ decrease in cell survival when cultures were treated with 2 mM of PS and 30 min of irradiation with visible light at a fluence rate of 30 mW cm^{-2}. For the Gram-positive bacterium *S. mitis*, a higher photoinactivation was found after irradiation, but in this case the order was $\mathbf{26c} > \mathbf{26c} > > \mathbf{26a}$. Here, photosensitization of *S. mitis* by **26c** caused a ≈ 4 log$_{10}$ reduction in cellular viability for cultures treated with 1 μM of

Chemistry–A European Journal

Review

doi.org/10.1002/chem.202002703

**Chemistry
Europe**

European Chemical
Societies Publishing

sensitizer and 30 min of irradiation. Considering these results, **26b** and **26c** may be more active PSs, but their effectiveness to accomplish lethal photosensitization of bacteria was reduced in the presence of human erythrocytes and human blood plasma.

Whereas positively charged Pc derivatives show a broad spectrum of activity, neutral and anionic Pcs still hold some affinity for Gram-positive bacteria. In a comparative study with cationic tetrakis-(3-methylpyridyloxy)- and anionic tetrakis-(4-sulfophenoxy)-phthalocyanine Zn^{II}, Mantareva et al. showed that the cationic Pc effectively inactivated Gram-positive *S. aureus* (no survival, 1.5 μM, 50 mW cm^{-2}, 10 min) and Gram-negative *P. aeruginosa* (6 μM, 100 mW cm^{-2}, 10-min), whereas the anionic derivative showed only some effectivity against Gram-positive *S. aureus* ($\approx 4 \log_{10}$ reduction, 6 μM, 100 mW cm^2, 10 min).[48] Similar studies performed with the anionic tetra-sulfonated phthalocyanine, the neutral tetra-diethanolamine phthalocyanine, and the cationic pyridinium phthalocyanine by Durantini et al. showed that the latter efficiently photo-inactivated the Gram-negative *E. coli* and *P. aeruginosa* and the Gram-positive *E. seriolicida*, but the same bacteria were unaffected by the neutral or anionic Pcs under the same irradiation conditions and the concentrations.[49] Other researchers in related areas have reported a neutral methylsulfonyl ZnPc with a high singlet oxygen quantum yield of 0.71 was found to be active against Gram-positive *S. aureus* ($>6 \log_{10}$ reduction, 5 μM, 45 J cm^{-2}), but, as expected for non-cationic PSs, it could not significantly kill Gram-negative *E. coli*.[50]

As a result of electrostatic repulsion molecules having negatively charged substituents, such as zinc octacarboxyphthalocyanine ($\Phi_\Delta = 0.57$) have almost no affinity to bacterial cells. By comparison, zinc octakis(pyridiniomethyl) phthalocyanine ($\Phi_\Delta = 0.45$), which has an identical central atom and a similar Φ_Δ, does have photobactericidal activity, indicating that the positive charge at the macrocycle periphery crucially affects *E. coli* photoinactivation.[51]

In recent years, synthesizing asymmetric Pcs started attracting attention after studies showed that PSs with an amphiphilic substitution pattern have higher activity than their symmetric analogues; while positively charged groups promote interaction with the bacterial cell outer membrane, the hydrophobic part may direct the PS to the interior of the cell. Several strategies for synthesizing asymmetric Pcs have been described in the literature.[52] Using a statistical condensation method, we recently showed that 2,4,6-tris(*N*,*N*-dimethylaminomethyl) phenoxy-substituted ZnPcs bearing none, three or six thiophenyl moieties could be readily synthesized.[53] Upon introducing the thiophenyl groups, the singlet oxygen quantum yield was increased from 0.61 for **27b** to 0.76 for **28** and 0.81 for **29**. For the first time, we showed that a PS's photobiological activity depended on the flexibility of the molecule rather than its ability to generate ROS. At a 1 μM concentration, light activation of **27b** and **28** resulted in a >5 log reduction of viable *E. coli* with a light dose of 18 J cm^{-2}. When **29** was tested under the same conditions, the colony forming units were reduced by $<2 \log_{10}$. At the same time, the Yoon group published an interesting study showing that a non-quaternized

derivative of **27b** was able to self-assemble into nanodots that generate ROS via the Type I mechanism.[54] A nano-PS concentration of 50 nM caused a 100% reduction of *E. coli*. Moreover, concentrations lower than 10 nM reduced the viability of Gram-positive *S. aureus*. As an extension of this work, we synthesized a metal-free derivative **27a** and compared its activity with **27b**.[55] Photophysical measurements showed that at neutral pH **27a** could not generate ROS via the Type I mechanism, however pH regulated increase of $^1O_2$ production was observed ($\Phi_\Delta = 0.02$ when pH 7.6 and $\Phi_\Delta = 0.22$ when pH 4.6). As expected, under the same irradiation conditions, **27a** was less active than **27b** against bacteria in both the planktonic and biofilm states. DFT-optimized structures of monomers and different types of dimers (H-bonded for **27a** and metal-ligand coordinated for **27b** and π–π stacked dimers for both) were compared, indicating that stabilization energy of the dimer where -N(Me)$_2$ group is coordinated to the zinc centre of neighbouring macrocycle is significantly higher. These results showed that the formation of metal–ligand coordinated active aggregates for **27b** compete well with the persistent π–π stacked inactive aggregate formation. This was not the case for metal-free counterpart **27a**.

Formation of self-assembled photoactive nanodots with aggregation-enhanced photodynamic effect was recently described by Lee et al.[56] The authors showed that 3-{*N*-(4-boronobenzyl)-*N*,*N*-dimethylammonium} phenoxy-substituted zinc(II) phthalocyanine can generate approximately 13 times higher ROS than methylene blue through both Type I and Type II photochemical mechanisms. Upon incubation of the PS with representative common and antibiotic-resistant bacterial strains of *S. aureus* and *E. coli* a significant decrease in bacterial colonies was observed ($\approx 100\%$ reduction when 50 nM of PS and laser irradiation of 0.4 W cm^{-2} for 10 min are applied).

As a key component of a low-symmetry Pc derivative for aPDT was prepared by conjugating ZnPc-COOH with a penta-lysine amino acid.[57] The cationic charge of ZnPc-(Lys)$_5$ enabled high uptake by *P. gingivalis* and *E. coli* compared to tetra sulfonate ZnPc. Further, in vitro studies of ZnPc-(Lys)$_5$ at a concentration of 1–20 μM significantly reduced the viability of Gram-negative bacteria when irradiated with 670 nm light at 6 J cm^{-2}. Further studies showed that microorganisms involved in skin bacterial infections *P. acnes* and *S. aureus* could also be efficiently inactivated.[58] For a series of oligolysine-conjugated ZnPcs, Ke et al. studied the effect of the lysine chain length on aPDT activity. They found that the efficacies of di-α-substituted ZnPcs to generate ROS were similar ($\Phi_\Delta = 0.86$–0.89), but the electronic absorption and fluorescence spectra showed that the derivative with four lysine units (**31**) was less aggregated than the derivatives with two units (**30**) and eight units (**32**). aPDT activity of all conjugates was determined against different Gram-positive and Gram-negative strains and expressed as the amount of PS needed to cause a 4 log reduction after 1 h incubation and irradiation ($\lambda > 610$ nm, 40 mW cm^{-2}, 48 J cm^{-2}). All conjugates showed good activity against *S. aureus* ATCC BAA-43 (24–39 nM), but **30** and **31** were more active against *S. aureus* 25923 (17 nM and 15 nM, correspondingly) than **32** (90 nM). To inactivate *E. coli* and *P. aeruginosa*, much higher

concentrations were need. The conjugate with the longest chain length, **32** (0.8 μM), was more active against *E. coli* than **30** (21.1 μM) and **31** (2.3 μM). *P. aeruginosa* was only inactivated with **31** (16.1 μM) (Figure 7).

Separating the hydrophobic and hydrophilic parts of a Pc was explored using two differently functionalized isoindol units.[59] ABAB-type Pcs functionalized with pyridines **33** or tertiary amines **34** were isolated and quaternized to achieve water solubility. Measurements of the singlet oxygen quantum yield by direct observation of the $^1O_2$ phosphorescence at 1275 nm in methanol showed that **34** had a lower Φ_Δ (0.35) than **33** (0.49). When comparing the aPDT activity on Gram-positive *S. aureus* and Gram-negative *E. coli* upon red light irradiation (33 J cm^{-2}), 0.1 μM of **33** and 0.5 μM **34** were needed to achieve a 3 log reduction of *S. aureus*. For comparable inactivation of *E. coli*, 10 μM of either PS was required.
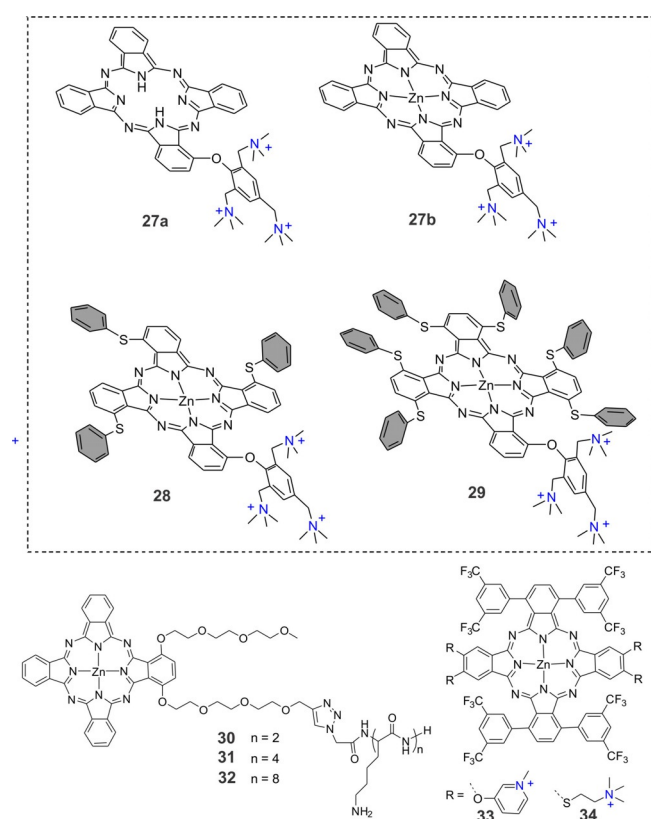

Figure 7. Structures of low-symmetry ZnPcs used in aPDT.

3.3. Phthalocyanines containing other metal centres

Besides the widely used silicon(IV) and zinc(II) Pc derivatives, Pcs containing other metal core atoms also display photosensitizing activity and have been used in aPDT. For example, commercially available aluminium disulfonated phthalocyanine (Photosens, **35**, Figure 8a) has been primarily used to treat various oncological indications and age-related macular degeneration. In 1995, Wilson et al. found that methicillin-resistant *S. aureus* could be significantly inactivated by Photosens and

light even in the presence of horse serum.[60] However, another study on 16 epidemic MRSA strains indicated that photodynamic inactivation with Photosens could not be achieved regardless of the growth phase of the organism; scavengers of singlet oxygen and free radicals protected the bacteria from inactivation.[61]

Nonell and co-workers recently studied dendrimer-encased PSs with four or eight positive charges and varying coordinating metals (zinc or ruthenium, Figure 8a).[62] In terms of producing $^1O_2$, the dendrimeric ZnPc **36** showed the highest value ($\Phi_\Delta = 0.12$ in deuterated water), which was almost two orders of magnitude higher than for **38** ($\Phi_\Delta = 0.02$). However, the $^1O_2$ sensitizing capacity of novel cationic ruthenium Pcs **37** and **39** remained the same ($\Phi_\Delta = 0.02$). The photodynamic inactivation studies against *S. aureus* and *E. coli* indicate that these compounds do not show improved photoinactivation. While **36** and **38** achieved a microbial reduction of > 6 $\log_{10}$ (1 μM, 60 J cm^{-2}) against *S. aureus* and **37** achieved a reduction of 3 log CFU mL^{-1} (1 μM and 60 J cm^{-2}), for *E. coli* the effect was much lower; a 6 log CFU mL^{-1} reduction was achieved at 2.5 μM for **36** and 5 μM for **38** at a 30 J cm^{-2} light dose; **37** required harsher photodynamic conditions for a 5 log reduction (5 μM, 60 J cm^{-2}). Finally, dendrimeric **38** only accomplished a modest 2 log CFU mL^{-1} reduction under the more extreme conditions of 50 μM and 100 J cm^{-2}. In another study, Saki et al.[63] examined the antimicrobial activities of five metallo-(Cu, Co, Zn, Ga and In) or non-metallo- octasubstituted Pc derivatives bearing diethylaminophenoxy- and chloro-substituents at peripheral positions. Disc diffusion and microdilution assays showed that among all the tested Pcs, only positively charged quaternized phthalocyanine molecules containing Ga and In metal centres showed antimicrobial activity against *E. coli* and *B. subtilis*.

Metal Pcs containing alkylated pyridoxy groups at the peripheral positions and different metals (Zn, Al, Ga, In, Si and Ge) at the centre of the Pc core were systemically studied by Mantareva et al.[64] Concerning singlet oxygen quantum yields, Pcs with metal ions with closed p or d electron configurations, such as Zn^{II} and Si^{IV}, had the highest Φ_Δ values, 0.41 and 0.68, respectively. Al, Ga, and In Pcs exhibited values between 0.36 and 0.16. Photodynamic inactivation with the water-soluble, cationic tetra-methylpyridyloxy- and octa-methylpyridyloxy-substituted GaPc[65] was investigated towards several bacterial strains (*S. aureus*, *E. faecalis* and *P. aeruginosa*) at relatively low concentrations (1–3 μM) and soft laser irradiation (60 mW cm^{-2}, 15 min). Complete photoinactivation was observed for the Gram-positive bacterial strains, while, for the same treatment conditions, the Gram-negative *P. aeruginosa* was inactivated with only a 2 $\log_{10}$ reduction. Whereas replacing Zn with Ge increased uptake of Pc by the bacterial cells and in some cases also increased activity, an Si containing Pc with the same substitution pattern showed decreased the aPDT effect when all non-bound Pcs were removed from the solution.[48,66] Analogous complexes of Al, In and Ge were evaluated to be unsuitable for aPDT. A study comparing PdPc **40** with tetra-pyrodoxy-substituted AlPc and ZnPc showed photoinactivation of Gram-negative *A. actinomycetemcomitans* with a
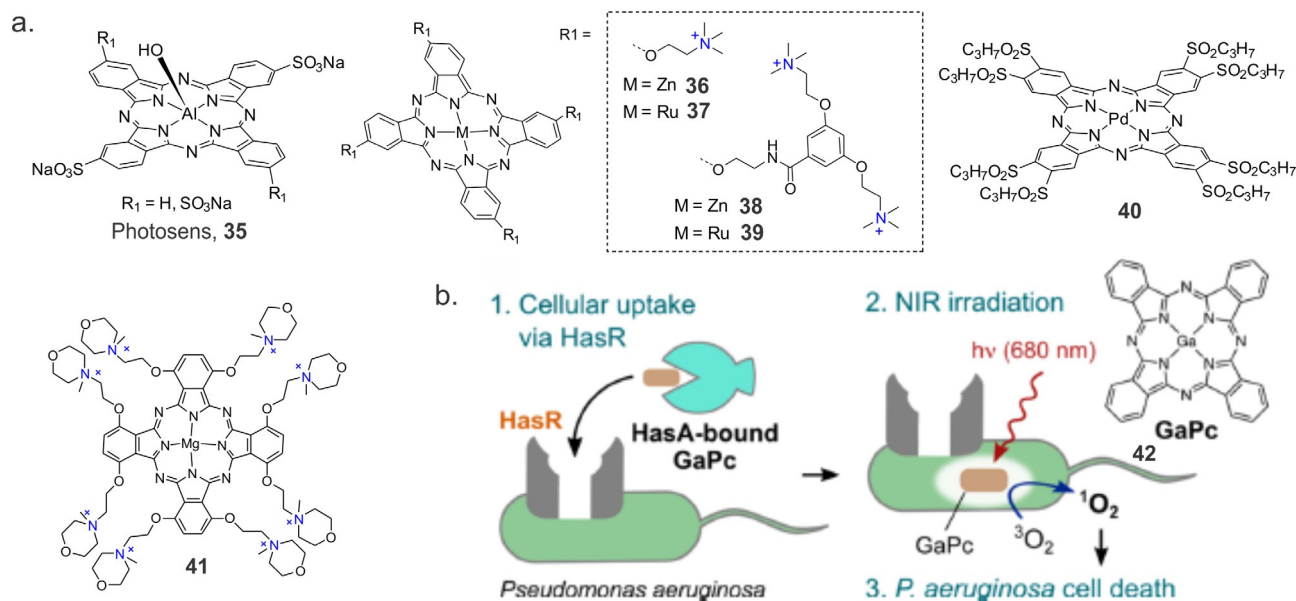
Chemistry–A European Journal

Review
doi.org/10.1002/chem.202002703

Chemistry Europe
European Chemical
Societies Publishing

Figure 8. (a) Chemical structures of some Pc-based systems used in aPDT. (b) Schematic representation of GaPc **42** uptake by *P. aeruginosa* by its heme acquisition system and photosensitization process. Reproduced with permission from Ref. [70]. Copyright 2017, American Chemical Society.

$4\log_{10}$ reduction after treatment with PdPc and with a 1.5–2 log reduction after treatment with AlPc.[67] Complete photoinactivation was observed after treatment with ZnPc at the same concentration and mild light irradiation (6.0 μM, 100 mW cm^{-2}, 15 min).

An octaiodide salt of MgPc with *N*-methyl morpholinium-ethoxy substituents in non-peripheral positions was synthesized by the Goslinski group (Figure 8a).[68] As expected, Φ_{Δ} for **41** in DMSO (0.12) and DMF (0.14) were lower than that for unsubstituted ZnPc. Nevertheless, at 100 μM concentration, **41** resulted in a $\approx 5\log_{10}$ reduction of representative Gram-positive and Gram-negative bacteria. However, the effectiveness of photodynamic inactivation decreased dramatically as the PS concentration decreased. There was no or little effect of **41** at 10 μM and 1 μM concentrations.

Recently an interesting strategy was developed by Shisaka et al., whereby the extracellular heme acquisition system protein A (HasA) was used to accumulate water-insoluble GaPc into the intracellular space of *P. aeruginosa* via the protein recognition of HasA

by the outer membrane receptor HasR (Figure 7b).[69] An irradiation time of only 10 min at a light irradiance of 10 mW cm^{-2} was sufficient to sterilize over 99.99% of bacteria when **42** was used as PS. This strategy shows that water-soluble protein carriers may be able to successfully deliver PS to target bacteria.

3.4. Supramolecular and polymer-based carrier systems

In recent years, an increasing number of researchers have considered polymer-based systems as PS carriers for aPDT.[70] This is particularly true for Pc-based PSs due to their inherent hydrophobicity and lack of solubility in biological media. The most common carrier systems are liposomes and micelles,[71]

but carbohydrates like cyclodextrins or polymerosomes are also used for drug delivery.[72]

Miretti et al. studied the ability of ZnPc loaded into dipalmitoylphosphatidylcholine-cholesterol-based liposomes to photoinactivate *M. tuberculosis*.[73] They found that a light dose of 150 J cm^{-2} generated a reduction of 5.7 and 2 $\log_{10}$ CFU mL^{-1} of drug-susceptible and drug-resistant strains, respectively. In another study, a cationic liposome formulation of aluminium-chloridephthalocyanine (AlClPc) was used to inactivate cariogenic bacteria in carious lesions.[74] The interaction of cariogenic bacteria and the liposome vesicles increased when positive superficial charges were present, leading to a significant mean reduction of 82% of viable cells after aPDT. In a different study, Ribeiro et al. studied the photodynamic antimicrobial effect of AlClPc encapsulated in cationic and anionic nanoemulsions (NE) and free AlClPc diluted in organic solvent.[75] The cationic NE-AlClPc and free AlClPc promoted photokilling of methicillin-susceptible and methicillin-resistant *S. aureus* when irradiated with a light fluence of 25 and 50 J cm^{-2}, respectively. Anionic NE-AlClPc in combination with the lower light fluence did not differ significantly from the negative control.

Recently, we prepared and characterized low-symmetry SiPc derivative **43** bearing an adamantly moiety that was able to anchor the PS on β-cyclodextrin vesicles (CDV) via the formation of host–guest complexes (Figure 9a).[76] Though binding of the PS to the CDV contributed to the reduced aggregation and slight increase of singlet oxygen quantum yield from 0.17 to 0.21 in an aqueous environment, the photosensitizing ability against methicillin-resistant *S. aureus* USA300 was not significantly affected. High-level bacterial inactivation ($\approx 7\log_{10}$ reduction, 108 J cm^{-2}) was observed with both the free and bound forms, indicating that suppressing the aggregation of PS compensates for its binding to the CDV when delivering the PS to the microorganism.
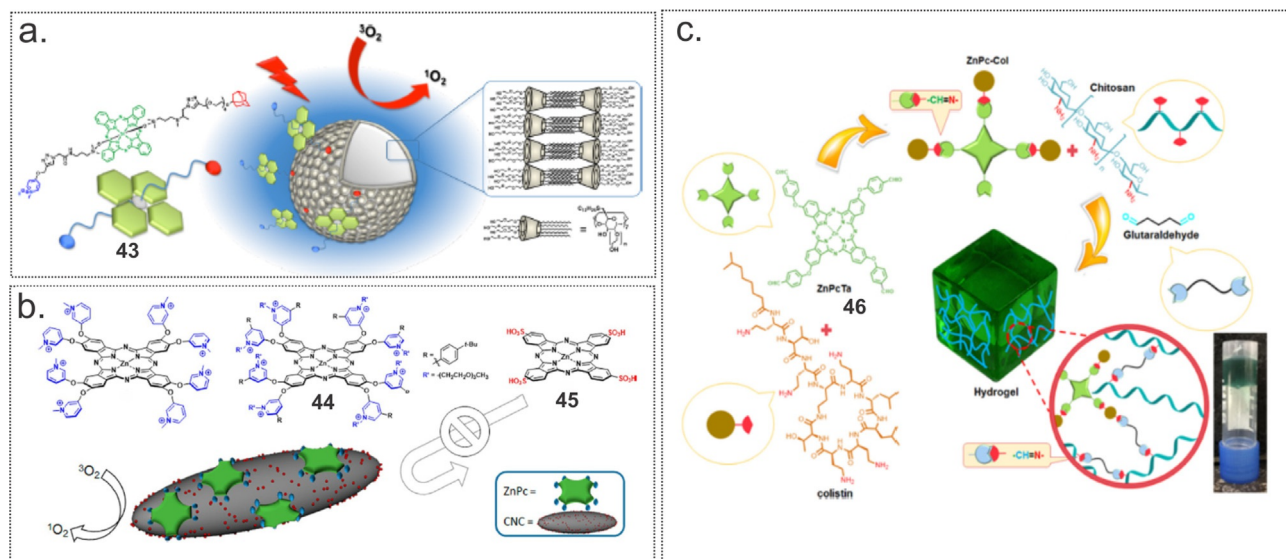
Chemistry–A European Journal

Review
doi.org/10.1002/chem.202002703

Chemistry Europe
European Chemical
Societies Publishing

Figure 9. (a) Schematic representation of cyclodextrin vesicles decorated with a tailored SiPc-based PS. Reproduced with permission from Ref. [77]. Copyright 2016, American Chemical Society. (b) Chemical structure of the cationic **44** and the anionic **45**. Schematic representation of ZnPc immobilized supramolecularly onto the surface of sulfate-decorated cellulose nanocrystals. Reproduced with permission from Ref. [78]. Copyright 2017, Wiley-VCH. (c) Schematic representation of the ZnPc **46**-colistin-containing hydrogel. Reproduced with permission from Ref. [80]. Copyright 2019, Elsevier.

Using electrostatic attraction as a driving force, the Torres group obtained a nanomaterial composed of octa-cationic ZnPc **44** and anionic cellulose nanocrystals (Figure 9b).[77] Anionic ZnPc **45** was employed as a negative control. The efficacy of obtained hybrid materials for photoinduced $^1O_2$ production was measured and compared with that of the corresponding free ZnPc. Contrary to what was expected, the biohybrids showed almost no $^1O_2$ photoproduction in any solvent. However, the photodynamic inactivation properties of these new biohybrids against *S. aureus* and *E. coli* outperformed those of their free ZnPc counterparts. Only a few J cm^{-2} reduced the viability of *S. aureus* by 6 logs and *E. coli* by 3 logs CFU using a 0.5 μM concentration; complete eradication (i.e., an 8 log$_{10}$ and a 6 log$_{10}$ CFU reduction for *S. aureus* and *E. coli*, respectively) were achieved at 3 μM and 64 J cm^{-2}. Free compounds were 3–4 logs less effective.

The photodynamic effect of immobilized PSs was studied by Bonnett et al. in 2006.[78] ZnPc-tetrasulfonic acid was covalently attached to chitosan via a sulfonamide linkage, and membranes for water disinfection were fabricated with or without nylon as an additive. Experiments performed with 10^{-5} cells mL^{-1} of *E. coli* showed a > 2 log$_{10}$ reduction, indicating that these types of systems can be used to lower microbial levels in water flow systems. In another study, Bayat and Karimi prepared a ZnPc-incorporated chitosan hydrogel as a new antibacterial system (Figure 9c).[79] To increase the practical advantages of ZnPc and improve interactions with the surface of Gram-negative bacteria, it was conjugated to colistin (ZnPc-Col). Furthermore, the authors used glutaraldehyde as a crosslinking agent. The singlet oxygen yield of the hydrogel with 25% w/w glutaraldehyde was much smaller (ZnPC-Col 20% w/w, $\Phi_\Delta = 0.19$), than ones with 15% w/w glutaraldehyde (ZnPC-Col 20% w/w, $\Phi_\Delta = 0.77$) and (ZnPC-Col 10% w/w, $\Phi_\Delta = 0.64$). The in vitro aPDT effect of the hydrogel with the highest

Φ_Δ value was assessed against a colistin-sensitive *P. aeruginosa* strain by a CFU assay; results showed that it caused a 3.32 and 2.76 log$_{10}$ reduction with and without laser irradiation for 10 min, respectively. Treatment with 15 min laser irradiation led to dramatically decreased viability (a 4.69 log$_{10}$ reduction of CFU mL^{-1}).

Many polymer-based systems have been applied as antibacterial coatings. In 2017, we reported a new concept for designing responsive materials with photobactericidal activity.[30] We used a boronic acid-functionalized PS that formed reversible bonds with hydroxyl groups of polyvinyl alcohol, which led to the formation of a hydrogel (Figure 10a). Cover slips coated with this material showed light-activated antibacterial properties and an extent of inactivation of uropathogenic *E. coli* bacteria was correlated with the amount of PS released from the hydrogel.

To increase the antimicrobial efficacy of an ε-polylysine coated cellulose fabric, Huang and co-workers covalently linked mono-substituted β-carboxy phthalocyanine zinc as a PS for aPDT (Figure 10b).[80] Non-functionalized fabric without irradiation was able to reduce the viability of both Gram-negative *E. coli* and Gram-positive *S. aureus* bacteria by ≈80%. Some increase in activity was observed upon irradiation (150 mW cm^{-2}, 40 min). Growth of 99% *E. coli* and 98% of *S. aureus* were inhibited.

In another study, Xu and co-workers synthesized zinc(II)monoamino Pc, which was conjugated to poly(glycidyl methacrylate) via a ring-opening reaction (Figure 10c).[81] When dispersed in aqueous solution, self-assembled nanoparticles (PGED-Pc NPs) were formed. Photophysical measurements showed that PGED-Pc NPs generated mainly superoxide/H$_2$O$_2$ instead of the expected $^1O_2$. Nevertheless, obtained NPs were able to inactivate both Gram-negative and Gram-positive bacteria in aqueous solutions, with a minimum bactericidal con-
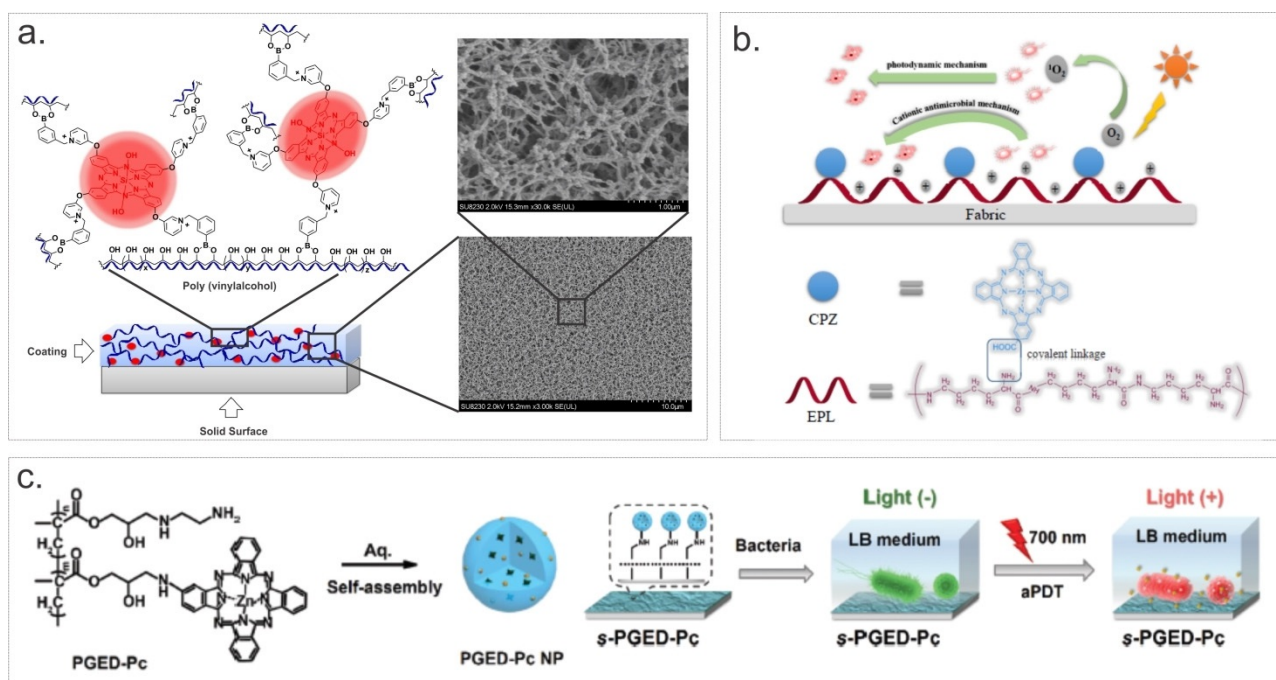
Figure 10. (a) Polyvinyl alcohol-SiPc-based coating and SEM images of swollen and freeze-dried hydrogel coatings. Reproduced with permission from Ref. [30]. Copyright 2017, Wiley-VCH. (b) Design strategy of a ZnPc-ε-polylysine fabric material with dual antimicrobial mechanisms. Reproduced with permission from Ref. [81]. Copyright 2017, Elsevier. (c) Schematic illustration of the formation of nanoparticles composed of ZnPc-conjugated poly(glycidyl methacrylate) and its application for the engineering of self-sterilizing surfaces. Reproduced with permission from Ref. [82]. Copyright 2019, The Royal Society of Chemistry.

centration of 128 µg mL^{-1} for *E. coli* and 4 µg mL^{-1} for *S. aureus*. As concluded from the corresponding analysis, the generated ROS induced the disruption of bacterial envelopes, the inactivation of vital enzymes, and the degradation of genomic DNA. Furthermore, the PGED-Pc NPs were shown to be easily immobilized onto aldehyde-modified glass slides via a Schiff-base reaction, leading to the formation of self-sterilizing surfaces effective against both Gram-negative *E. coli* (91% inactivation) and Gram-positive *S. aureus* (96% inactivation).

In another study, a remarkably simple and straightforward method was used by Efimov and co-workers to prepare photoactive material; qualitative-grade filter paper was immersed into aqueous solutions of ZnPc with four quaternized pyridyl substituents for 10 min.[82] This material was able to inactivate over 99.996% of drug-resistant *C. albicans*, *S. aureus* and *E. faecalis* in just a 1 h exposure with consumer-grade fluorescent lamps and diodes.

Electrospinning is a simple and inexpensive method for the fabrication of nanofiber mats and in combination with suitable PS could be used to obtain photoactive antibacterial interfaces. In our recent study, we have reported a simple, low-cost, one-step fabrication of nanoscale patterns from the mixture containing poly(ethylene glycol) (PEG)-functionalized silicon(IV)-phthalocyanines (SiPcPEG$_2$ and SiPcPy$_4$PEG$_2$), PVA, and sebacic acid (Figure 11).[83] Both PS were able to efficiently generate ROS in water and dimethylformamide ($\Phi_\Delta = 0.35$ and 0.40 in DMF and $\Phi_\Delta = 0.23$ and 0.39 in H$_2$O correspondingly for SiPc-PEG$_2$ and SiPcPy$_4$PEG$_2$) and showed high activity against *S. aureus*, *S. warneri*, and *B. subtilis* ($>5 \log_{10}$ redaction for the

SiPcPEG$_2$ and $>3 \log_{10}$ redaction for the SiPcPy$_4$PEG$_2$, 1 µM, 9 J cm^{-2}). Obtained electrospun materials were also phototoxic against bacteria without being cytotoxic on human fibroblasts and, additionally, showed antifouling properties.

In 2015, the group of Mosinger used electrospinning to obtain polystyrene nanofiber materials with ionically bound tetracationic zinc(II) 2,9,16,23-tetrakis(*N*-methyl-pyridiumoxy)-phthalocyanine tetraiodide as PS.[84] To overcome short radius of ^{1}O$_2$ diffusion, additionally, nitric oxide photodonor was covalently grafted onto the material. Multifunctional nanofiber materials showed $>50\%$ inhibition of *E. coli* after irradiation by visible light.

3.5. Metal nanoparticle-based systems

Metal nanoparticles (NPs) have a relatively narrow size and shape distribution, high loading, slow degradation, a long period of activity in water dispersions, making them attractive for biomedical applications.[85] They can be used as delivery vehicles and upconversion tools; for example, irradiating NPs with relatively low-power radiation can lead to photo-stimulated reactions on the NP surfaces. New properties, such as enhanced generation of ROS, can arise in complexes formed of metal NPs with PSs. The Nyokong group systematically investigated systems where Pc derivatives were conjugated to different metal NPs; easy surface modification of the NPs was achieved by thiol chemistry. In 2013, they reported on the axial coordination of zinc phthalocyanine and bis-(1,6-hexanedithiol) silicon phthalocyanine to silver and gold NPs.[86] The ZnPc-
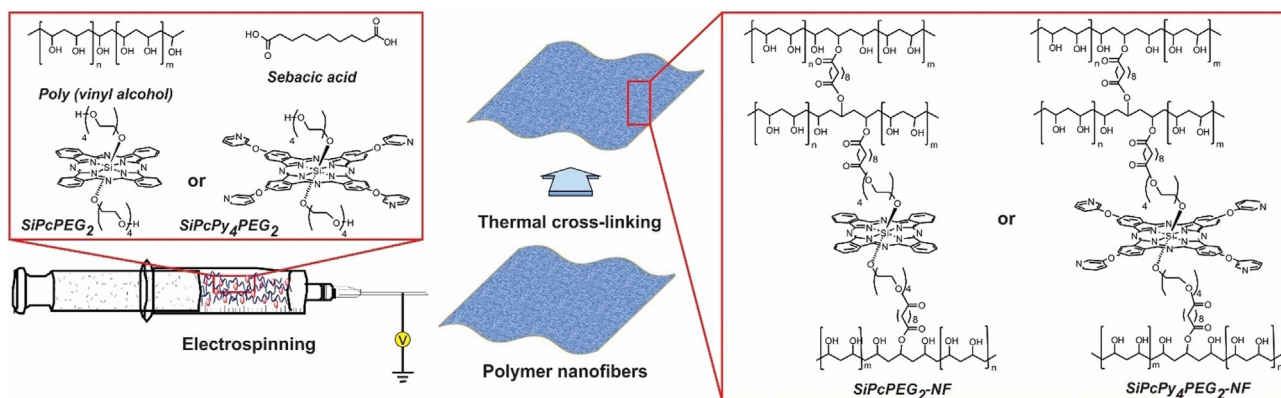
Chemistry–A European Journal

Review

doi.org/10.1002/chem.202002703

**Chemistry
Europe**
European Chemical
Societies Publishing

Figure 11. Schematic representation of electrospinning of nanofibers using SiPcPEG2 and SiPcPy4PEG2 and possible crosslinking process with premixed components. Reproduced with permission from Ref. [84]. Copyright 2020, American Chemical Society.

AgNP conjugates gave the highest singlet oxygen quantum yield (0.63), followed by ZnPc-AuNPs (0.58) and ZnPc (0.56). The SiPc complex gave the lowest singlet oxygen quantum yield, with a value of 0.44, which was increased upon coordination to NPs; the SiPc-AgNPs had a value of 0.50 and SiPc-AuNPs 0.53. The results of antimicrobial activities were presented in terms of percentage bacterial growth; the MIC for SiPc was 3.13 μM against both bacteria (*S. aureus* and *B. subtilis*) and 6.25 μM for ZnPc under illumination with light. Higher antimicrobial inhibition was observed in the presence of Pc-NPs, with SiPc-AgNPs showing MIC <0.195 μM. In a further study, the same group used anisotropic AuNPs (rods and bipyramids) conjugated to positively charged AlPc as aPDT agents (Figure 12a).[87] As expected, an increase of singlet oxygen quantum yield from 0.12 (single molecule) to 0.23 and 0.24 (AlPc-AuNPs) was recorded. Irrespective of the shape of the conjugated nanoparticles, enhanced photoinactivation against *E. coli* upon irradiation was observed. AlPc alone (20 μM) showed a 2.51 $\log_{10}$ reduction, while a 3.32 $\log_{10}$ reduction was observed with bipyramids and a 3.71 $\log_{10}$ reduction was observed with nanorods (light intensity at 691 nm was 3.22×10^{17} photons cm^{-2} s^{-1}).

Since low-symmetry Pcs have a higher binding specificity compared to their symmetrical counterparts, *tris*{11,19,27-(1,2-diethylaminoethylthiol) −1,2 (caffeic acid) phthalocyanine} Zn (ZnMCafPc, **47**) and tris{11,19,27-(1,2-diethylaminoethylthiol)-2-(captopril) phthalocyanine}Zn (ZnMCapPc, **48**) were synthesized and used for one point of attachment for the Pcs and glutathione-decorated AgNPs via a coupling reaction (Figure 12b).[88] The fluorescence quantum yields of NP conjugates decreased from 0.09 to 0.05 due to energy transfer from phthalocyanines in the excited state to the metal nanoparticles. In contrast, the singlet oxygen quantum yield increased upon conjugation, to 0.57 and 0.52 obtained for the ZnMCapPc-GSH-AgNPs and ZnMCafPc-GSH-AgNPs, respectively. Due to the synergistic effect brought about by the AgNPs and the Pc, a significant decrease in survival of *E. coli* cells was observed, but free Pcs was found to be more toxic without illumination than the conjugates.

The same group studied the conjugation of various shapes of silver nanoparticles to mono cysteinyl substituted metal phthalocyanines (OH)$_2$GeMCsPc, OTiMcPc, SnMCsPc and ZnMCsPc.[89] A slight improvement in singlet oxygen quantum yield was observed in the presence of all the AgNPs in some cases, suggesting an enhanced intersystem crossing to the triplet state. The spherically shaped AgNPs showed the best antibacterial activity, followed by the triangular shaped AgNPs when compared to their counterparts without MPc complexes. In the absence of light, the (OH)$_2$GeMCsPc (without AgNPs) gave the highest dark antibacterial activity against *S. aureus*, whereas an enhanced bacterial activity was observed in the light (90 min irradiation) when AgNPs were combined with phthalocyanines. Inactivation efficacy followed the order Sn $<$ OTi $<$ Zn $<$ (OH)$_2$Ge.

In a different study, zinc and indium Pcs bearing carboxyl groups were synthesized and conjugated to silver triangular nanoprisms.[90] Conjugation of nanoparticles increased singlet oxygen quantum yields of both Pcs (from 0.32 to 0.41 for ZnPc and from 0.46 to 0.48 for InPc). The conjugates were further embedded in asymmetric polymer membranes that also generated singlet oxygen. The Pcs and conjugates were then studied for aPDT activity against *S. aureus*, with ZnPc and ZnPc -AgNP showing good activity (50% reduction, 5 μM, 1.8 J cm^{-2}). The activity of InPc and InPc-AgNP was lower under the same test conditions ($\leq 50\%$ reduction). The low activities of the corresponding InPc were attributed to their degradation in aqueous media.

To enhance interaction between PS and microoganisms, Nyokong and co-workers synthesised conjugates of ZnPc with positively charged polylysine (PL) by reacting tetrasulfonyl-chloride ZnPc with PL at room temperature without using any coupling agents (2-ε-PL, $\Phi_\Delta = 0.22$) or by reacting 4-tetrakis-(5-trifluoromethyl-2- pyridyloxy)phthalocyaninato zinc(II) with PL after activating carboxylic groups with *N,N*-dicyclohexylcarbodiimide (3-ε-PL, $\Phi_\Delta = 0.11$).[91] The conjugates were further attached to AuNPs and AgNPs to study the effect of NPs on the antibacterial activity. The MIC$_{50}$ value for inactivation of *S. aureus* for 2-ε-PL (0.187 μM) upon irradiation (39.6 mW cm^{-2}, 10 min) was higher than for 3-ε-PL (0.046 μM) despite a lower

Chemistry–A European Journal

Review
doi.org/10.1002/chem.202002703

Chemistry
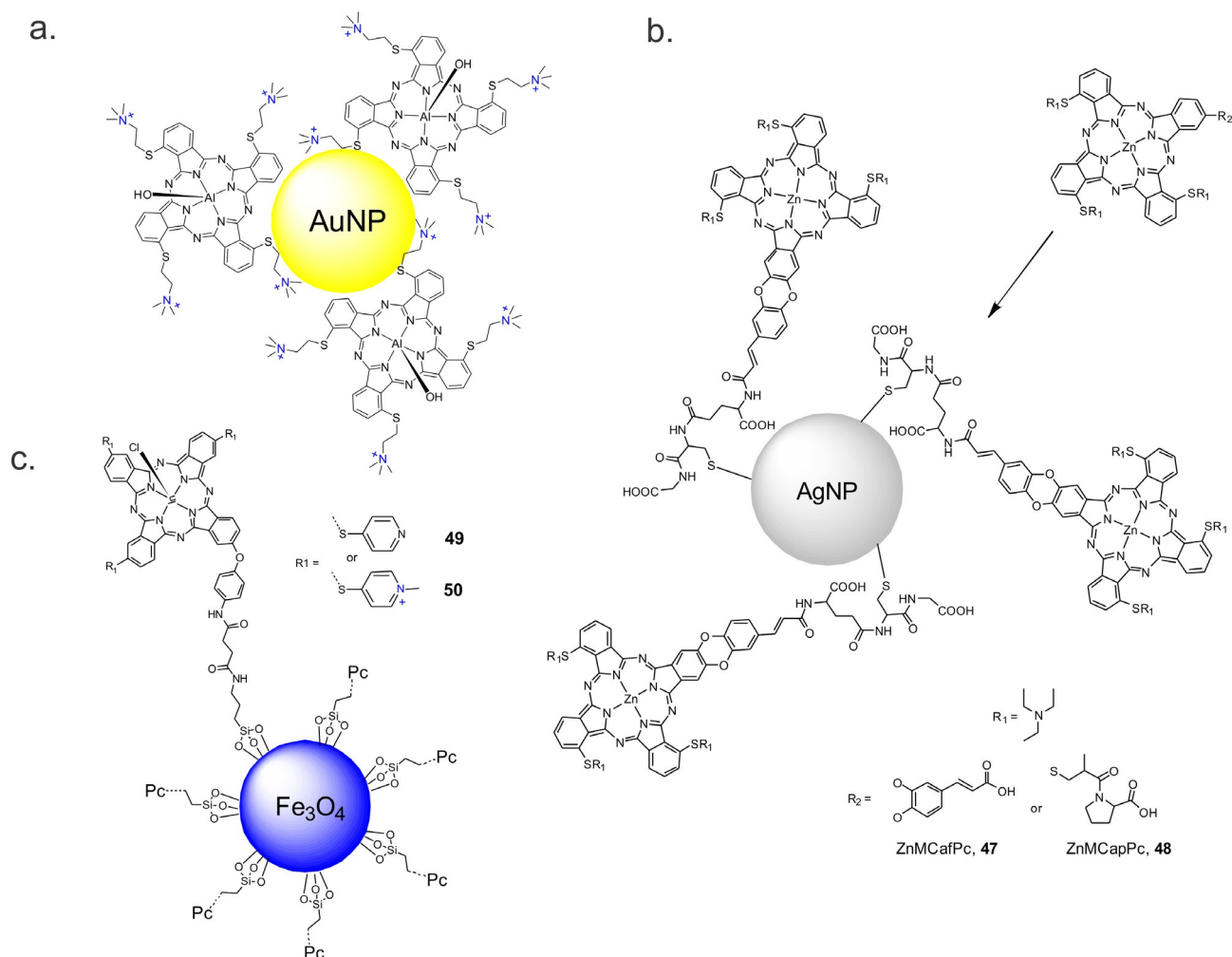**Europe**
European Chemical
Societies Publishing

Figure 12. Hypothetical structure based on the linking of a) AlPc to AuNP, b) ZnMCafPc **47** and ZnMCapPc **48** to AgNP and c) conjugation of magnetic nanoparticles and the photosensitizers **49** and **50**.

Φ_Δ of the latter, probably due to the amphiphilic nature of 3-ε-PL. Conjugation with AgNP and AuNP significantly increased activity of both conjugates ($MIC_{50} < 0.046$ for AuNPs and $MIC_{50} < 0.0058$ for AugNPs). The photophysicochemical properties and the aPDT activities of the recently reported zinc(II) tri (*tert*-butyl phenoxy) mono cinnamic acid-cys-AgNPs conjugates and the Pcs alone on *S. aureus* followed the same trend: The singlet oxygen quantum yield increased from 0.59 to 0.67 and the antibacterial activity increased (from a 6.12 log to a 8.06 log reduction for free ZnPc and ZnPc-AgNP, respectively, 120 min irradiation).[92]

When they are non-toxic and biocompatible, magnetic nanoparticles have the potential for use in various medical applications, such as magnetic resonance imaging, hyperthermia, drug delivery, and cell separation. In 2016, Osifeko et al. reported a study in which, for the first time, Pcs and magnetic nanoparticles (MNPs) were combined for aPDT.[93]

They conjugated a low-symmetry phthalocyanine 9(10), 16(17), 23(24)-tri-4-pyridylsulfanyl-2(3)-(4-aminophenoxy)-phthalocyaninato chloroindium(III), **49**, and its quaternized derivative, **50**, to carboxylic acid-functionalized Fe_3O_4 MNP (Fig-

ure 12 c). Φ_Δ values were found to be higher for **49** (0.44) compared to **49**-MNPs (0.35) but were higher for **50**-MNPs (0.31) than for **50** (0.26). The PSs were characterized, and their effectiveness on Gram-negative *E. coli* was studied. The cationic PS **50** showed a high efficiency (6.45 log reduction) at 14 mg L^{-1} when compared to the quaternized PS conjugated with the functionalized magnetic nanoparticles (4.39 log reduction, 200 mg L^{-1}). The non-cationic conjugate (**49**-MNPs) was not effective even at higher concentrations (0.8 log reduction).

3.6. Other Pc-functionalized nanomaterials

Carbon-based nanomaterials, such us carbon dots and nanotubes have attracted wide interest in biomedical research in recent years due to their excellent physical and chemical properties and ease of preparation and functionalization.[94] To improve the efficacy of aPDT application Openda et al synthesized nanoconjugates of graphene quantum dots (GQD) and novel acetophenone substituted unmetalated, zinc and indium Pcs.[95] Higher values for singlet oxygen generation was observed for ZnPc (0.72) and InPc (0.75), compared to H_2Pc (0.22).

Chemistry–A European Journal

Review
doi.org/10.1002/chem.202002703

Chemistry Europe
European Chemical
Societies Publishing

The capability of ZnPc and InPc to generate ROS was slightly increased upon conjugation to GQD (0.77 for ZnPc@GQD and 0.79 for InPc@GQD), while the value recorded for H_2Pc was still low (0.20). Antimicrobial activities of the Pcs and Pc@GQD conjugates were evaluated against Gram-positive *S. aureus*. Upon irradiation, with a red light at 670 nm for 60 min highest $\log_{10}$ reduction was observed for InPc@GQD (9.68), followed by ZnPc@GQD (3.77). In all other cases, $\log_{10}$ reduction was <3. Recently Das et al. have synthesized antibacterial hybrid nanomaterial by deposition of graphene oxide flakes on ZnPc-coated indium tin oxide substrates.[96] Interestingly, kelvin probe force microscopy revealed efficient inactivation of Gram-negative *E. coli* without photo-excitation. It was supposed that bacterial cell death is caused by rapid changes in the surface potential on the cell wall caused by charge-transfer between negatively charged cells and the electron-withdrawing surface.

Using bottom-up ''breath figure'' technique Zhou et al. have fabricated thin, self-assembled, honeycomb-patterned films composed of dodecyloxy-azo-ZnPcs.[97] Singlet oxygen sensor green was used to confirm generation of $^1O_2$. Antibacterial activity was tested against amoxicillin-resistant by depositing bacterial cell suspension on the film and then irradiating it with 0.4 $mw\,cm^{-2}$ white light for up to 4 h. In comparison to glass-slide, drop-cast ZnPc film could considerably reduce bacterial cell growth.

Another interesting study describing the effect of carbon nanorods on aPDT activity of polyfluoroalkyl substituted SiPc against Gram-negative *E. coli* was reported by Chen et al.[98] For the synthesis of the supermolecule first pyrene-labelled-β-cyclodextrin was attached to the sidewalls of nanotubes via π–π interaction. Further, host-guest chemistry between cyclodextrin and fluoroalkyl chains of SiPc was used to obtain the final material (Figure 13a). Singlet oxygen quantum yield of SiPc was reduced when bound to nanotubes from 0.494 to 0.0754, however, authors showed that upon light irradiation disassembly of nanomaterial occur and photophysical characteristics of SiPc were recovered. High antibacterial effect ($\approx 3\,\log_{10}$ reduction, 660 nm, 15 min, 120 $mW\,cm^{-2}$) was attributed to the synergistic effect of the photothermal effect of the nanotubes and aPDT activity of SiPc.

Nanometric graphene oxide-based material composed of reduced graphene oxide (rGO), silver nanoparticles (Ag), and bis(lysinato)zirconium(IV) phthalocyanine complex (ZrPc) was described by Gerasymchuk et al.[99] Antimicrobial activity of GO-ZrPc, rGO-Ag, and rGO-ZrPc-Ag composites were tested against *S. aureus, P. aeruginosa* and *E. coli*. For *S. aureus* MIC values of all composites were equal (320 $\mu g\,mL^{-1}$) in the dark conditions, but decreased two-fold for GO-ZrPc upon irradiation. Gram-negative bacteria were more sensitive to rGO-Ag in the dark (1.28 $mg\,mL^{-1}$). After NIR irradiation reduction of MIC values for Pc-functionalized composites was observed (320 $\mu g\,mL^{-1}$ for *P. aeruginosa* and 160 $\mu g\,mL^{-1}$ for *E. coli*).

Inorganic nanoparticles based on (alumino)silicates were also used as carriers of diverse Pc-based PSs. Hybrid photoactive nanomaterial containing Zeolite L crystals loaded with DXP (*N,N'*-bis(2,6-dimethylphenyl)perylene-3,4,9,10-tetracarbodiimide) and axially bound SiPc as PS was designed and syn-
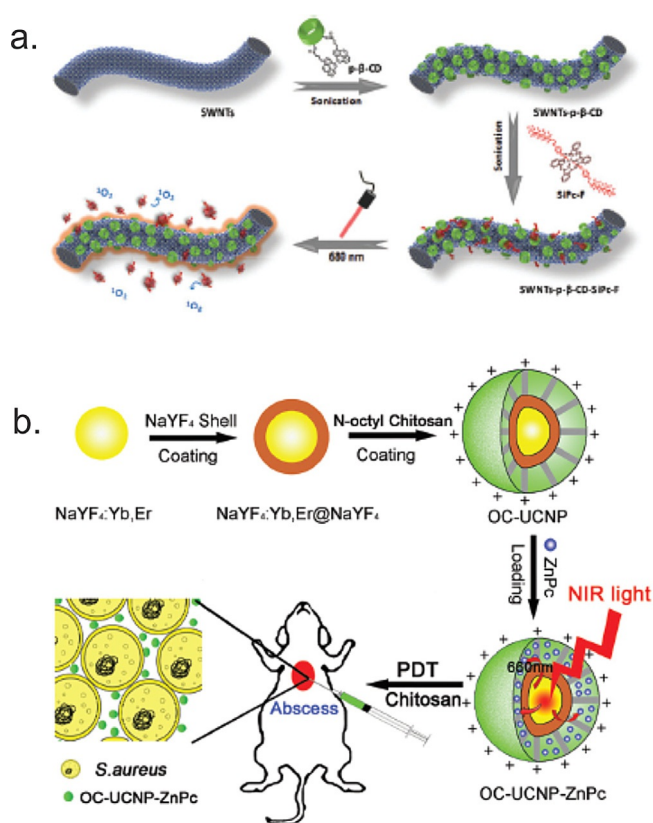

Figure 13. a) The schematic representation for the assembly process of single-wall carbon nanotubes with pyrene-labelled-β-cyclodextrin and SiPc. Reproduced with permission from Ref. [98]. Copyright 2019, The Royal Society of Chemistry. b) Schematic diagram of the synthesis of *N*-octyl chitosan-upconversion nanoparticle-ZnPc hybrid nanoconstruct and its antibacterial activity in vivo. Reproduced with permission from Ref. [103]. Copyright 2017, The Royal Society of Chemistry.

thesized by the group of De Cola.[100] The obtained material was able to target, label, and efficiently photoinactivate (up to 100% reduction of viability) Gram-negative *E. coli* and *N. gonorrheae*. To increase the stability of the system later Grüner et al. used disc shaped Laponite D nanoparticles and tetra-*tert*-butyl-substituted SiPc to obtain hybrid nanomaterial.[101] Despite low ROS generation ability ($\Phi_\Delta \leq 0.14$), obtained nanomaterial could inactivate up to 99% of Gram-positive bacterial species (*S. aureus* 6850, *S. aureus* USA 300, *S. aureus* Cowan I, and *E. faecalis*) when irradiated with the red light for 4 h (total radiant exposure: 144 $J\,cm^{-2}$).

Hybrid nanoconstructs with dual antimicrobial activity composed of β-NaYF4:23%Yb,2%Er@NaYF4 nanoparticles coated with cationic *N*-octyl chitosan and unsubstituted ZnPc were described by Li et al. in 2017 (Figure 13b).[102] Using diphenylisobenzofuran as ROS sensitive dye, authors showed that ROS production increased by increasing irradiation time and amount of ZnPc. Antimicrobial activity of nanomaterial at 125 $\mu g\,mL^{-1}$ concentration was studied against both Gram-positive (*S. aureus, S. epidermidis*) and Gram-negative (*E. coli, P. aeruginosa*) bacteria showing that decrease of colony-forming units occurs in dark and upon irradiation with 980 nm laser at 0.4 $W\,cm^{-2}$ intensity for 15 min. Series of core–shell mesopo-

Chemistry–A European Journal

Review
doi.org/10.1002/chem.202002703

**Chemistry
Europe**
European Chemical
Societies Publishing

rous silica-coated NaYF4:Yb:Er upconversion nanoparticles decorated with hydrophobic *tetra*-tert-butyl-substituted SiPc and different ligands ((3-aminopropyl)triethoxysilane, which was further modified with MeI, HOOC-TEG-COOH or HOOC-TEG-NH$_2$) were recently described by Grüner et al.[103] The authors showed that the ROS generation is dependent form the degree and type of functionalization. The highest value of 0.11 was obtained for the precursor containing only mesoporous silica shell. Antibacterial activities against *E. coli* and *S. aureus* showed that upon functionalization dark toxicity of the particles increased. Irradiation with a red light at 660 nm (108 J cm^{-2}) caused almost complete inactivation of *E. coli* and a considerable decrease in viability of *S. aureus* (6–7 log$_{10}$ reduction).

To enable fast and easy recovery of the nanomaterial group of Tomé prepared silica-coated magnet nanoparticles decorated with glycosylated Pc derivative.[104] Obtained material showed high efficacy for the photodynamic inactivation of *E. coli.*, due to the stronger interaction of the thioglucose units with the bacterial cell membrane. Complete inactivation of viable bacteria was achieved with ZnPc derivative at 20 μM concentration and 240 min of white light irradiation at 4 mW cm^{-2}.

4. Conclusion and Perspectives

As shown throughout this Review, phthalocyanine derivatives have become one of the most promising PSs for photodynamic inactivation of Gram-positive and Gram-negative bacteria, including resistant strains, due to their unique photophysical features. Different synthetic strategies have been developed to optimize the structure of PSs for certain applications. Despite myriad studies, identifying all the key features that are required for a "perfect" PS is not trivial. Some criteria are likely more important than others for optimizing PS performance. Though light absorption range and ROS quantum yield are important parameters, it seems that the interaction of a PS with the bacterial cell plays a substantial role in aPDT. Dedicated efforts from many laboratories have shown that introducing positive charges to the PS or conjugating the PS with positively charged polymers and nanoparticles ensures a broad spectrum of action and enhances overall efficacy. Encouraging results have been obtained in the field of Pc-based photoactive materials and nano-delivery systems, and I believe that many novel strategies will arise in the coming years, such as the use of microneedles to deliver PSs or the development of responsive systems that take advantage of specific internal and external triggers. Potent and cost-effective materials may be able to be fabricated using biodegradable and non-biodegradable polymers, and these materials will likely find applications in different fields of medicine and everyday life. Great progress has also been achieved over the past few decades in the development of metal nanoparticles decorated with Pc derivatives. These studies represent a good starting point for further developments that can help overcome some of the limitations of these systems regarding chemical and thermal susceptibility.

The knowledge we have gained from numerous studies is anticipated to facilitate the translation of aPDT into daily clinical practice. To reach this aim, PSs that can selectively accumulate in bacterial cells in vivo need to be designed and synthesized, and preclinical and clinical protocols need to be optimized.

Conflict of interest

The authors declare no conflict of interest.

[1] a) X. Ai, J. Mu, B. Xing, *Theranostics* **2016**, *6*, 2439–2457; b) K. C. Moore, *Photomed. Laser Surg.* **2013**, *31*, 563–564; c) M. R. Hamblin, Y. Y. Huang, *Handbook of Photomedicine*, CRC, **2013**.

[2] a) M. R. Hamblin, T. Hasan, *Photochem. Photobiol. Sci.* **2004**, *3*, 436–450; b) M. Wainwright, T. Maisch, S. Nonell, K. Plaetzer, A. Almeida, G. P. Tegos, M. R. Hamblin, *Lancet Infect. Dis.* **2017**, *17*, e49–e55; c) R. Yin, M. Hamblin, *Curr. Med. Chem.* **2015**, *22*, 2159–2185; d) Q. Jia, Q. Song, P. Li, W. Huang, *Adv. Healthc. Mater.* **2019**, *8*, 1900608.

[3] Y. Nitzan, M. Gutterman, Z. Malik, B. Ehrenberg, *Photochem. Photobiol.* **1992**, *55*, 89–96.

[4] a) J. O'Neill, *Tackling Drug Resistant Infections Globally: Final Report and Recommendations*, Review on Antimicrobial Resistance, London, **2016**, available online: https://amr-review.org/; b) United Nations Meeting on Antimicrobial Resistance, *Bull. World Health Organ.* **2016**, *94*, 638–639.

[5] a) M. R. Hamblin, H. Abrahamse, *Drug Dev. Res.* **2019**, *80*, 48–67; b) T. Maisch, S. Hackbarth, J. Regensburger, A. Felgenträger, W. Bäumler, M. Landthaler, B. Röder, *J. Dtsch. Dermatologischen Gesellschaft* **2011**, *9*, 360–366.

[6] M. DeRosa, *Coord. Chem. Rev.* **2002**, *233–234*, 351–371.

[7] S. Callaghan, M. O. Senge, *Photochem. Photobiol. Sci.* **2018**, *17*, 1490–1514.

[8] a) E. Alves, M. A. F. Faustino, M. G. P. M. S. Neves, A. Cunha, J. Tome, A. Almeida, *Future Med. Chem.* **2014**, *6*, 141–164; b) B. Ezraty, A. Gennaris, F. Barras, J.-F. Collet, *Nat. Rev. Microbiol.* **2017**, *15*, 385–396.

[9] M. R. Hamblin, H. Abrahamse, *Antibiotics* **2020**, *9*, 53.

[10] a) O. Raab, *Z. Biol.* **1900**, *39*, 524–546; b) R.-M. Szeimies, *Aktuelle Derm.* **2005**, *31*, 193–197.

[11] P.-C. Lo, M. S. Rodríguez-Morgade, R. K. Pandey, D. K. P. Ng, T. Torres, F. Dumoulin, *Chem. Soc. Rev.* **2020**, *49*, 1041–1056.

[12] G. Jori, C. Fabris, M. Soncin, S. Ferro, O. Coppellotti, D. Dei, L. Fantetti, G. Chiti, G. Roncucci, *Lasers Surg. Med.* **2006**, *38*, 468–481.

[13] D. K. Ng, *Future Med. Chem.* **2014**, *6*, 1991–1993.

[14] a) F. Dumoulin, M. Durmuş, V. Ahsen, T. Nyokong, *Coord. Chem. Rev.* **2010**, *254*, 2792–2847; b) *Phthalocyanines: Properties and Applications* (Eds.: C. C. Leznoff, A. B. P. Lever), Wiley-VCH, Weinheim, **1989**.

[15] a) H. Lu, N. Kobayashi, *Chem. Rev.* **2016**, *116*, 6184–6261; b) G. de la Torre, C. G. Claessens, T. Torres, *Chem. Commun.* **2007**, *2000*–2015; c) T. Torres, *J. Porphyr. Phthalocyanines* **2000**, *04*, 325–330.

[16] a) M. A. Pereira, M. A. F. Faustino, J. P. C. Tomé, M. G. P. M. S. Neves, A. C. Tomé, J. A. S. Cavaleiro, Â. Cunha, A. Almeida, *Photochem. Photobiol. Sci.* **2014**, *13*, 680–690; b) T. Maisch, R.-M. Szeimies, G. Jori, C. Abels, *Photochem. Photobiol. Sci.* **2004**, *3*, 907–917.

Chemistry–A European Journal

Review

doi.org/10.1002/chem.202002703

Chemistry
Europe
European Chemical
Societies Publishing

[17] a) F. Sperandio, Y.-Y. Huang, M. Hamblin, *Recent Pat. Antiinfect. Drug Discovery* **2013**, *8*, 108–120; b) A. Galstyan, U. Dobrindt, *J. Photochem. Photobiol. B* **2019**, *197*, 111554.

[18] S. I. A. Zaidi, R. Agarwal, G. Eichler, B. D. Rihter, M. E. Kenney, H. Mukhtar, *Photochem. Photobiol.* **1993**, *58*, 204–210.

[19] M. Dimaano, C. Rozario, M. Nerandzic, C. Donskey, M. Lam, E. Baron, *Int. J. Mol. Sci.* **2015**, *16*, 7851–7860.

[20] G. C. Taşkın, M. Durmuş, F. Yüksel, V. Mantareva, V. Kussovski, I. Angelov, D. Atilla, *J. Photochem. Photobiol. A* **2015**, *306*, 31–40.

[21] Z. Biyiklioglu, I. Ozturk, T. Arslan, A. Tunçel, K. Ocakoglu, M. Hosgor-Limoncu, F. Yurt, *Dye Pigment.* **2019**, *166*, 149–158.

[22] P. Sen, A. Sindelo, D. M. Mafukidze, T. Nyokong, *Synth. Met.* **2019**, *258*, 116203.

[23] İ. Ömeroğlu, E. N. Kaya, M. Göksel, V. Kussovski, V. Mantareva, M. Durmuş, *Bioorg. Med. Chem.* **2017**, *25*, 5415–5422.

[24] İ. Ömeroğlu, M. Göksel, V. Kussovski, V. Mantareva, M. Durmuş, *Macroheterocycles* **2019**, *12*, 255–263.

[25] C. Uslan, N. D. İşleyen, Y. Öztürk, B. T. Yıldız, Z. P. Çakar, M. Göksel, M. Durmuş, Y. H. Gürsel, B. Ş. Sesalan, *J. Porphyr. Phthalocyanines* **2018**, *22*, 10–24.

[26] P. Sen, T. Nyokong, *Polyhedron* **2019**, *173*, 114135.

[27] M. Managa, M. A. Idowu, E. Antunes, T. Nyokong, *Spectrochim. Acta Part A* **2014**, *125*, 147–153.

[28] A. Galstyan, J. Putze, U. Dobrindt, *Chem. Eur. J.* **2018**, *24*, 1178–1186.

[29] E. van de Winckel, B. David, M. M. Simoni, J. A. González-Delgado, A. de la Escosura, Â. Cunha, T. Torres, *Dye Pigment.* **2017**, *145*, 239–245.

[30] A. Galstyan, R. Schiller, U. Dobrindt, *Angew. Chem. Int. Ed.* **2017**, *56*, 10362–10366; *Angew. Chem.* **2017**, *129*, 10498–10502.

[31] A. Galstyan, D. Block, S. Niemann, M. C. Grüner, S. Abbruzzetti, M. Oneto, C. G. Daniliuc, S. Hermann, C. Viappiani, M. Schäfers, B. Löffler, C. A. Strassert, A. Faust, *Chem. Eur. J.* **2016**, *22*, 5243–5252.

[32] Y. Zhao, J.-W. Ying, Q. Sun, M.-R. Ke, B.-Y. Zheng, J.-D. Huang, *Dye Pigment.* **2020**, *172*, 107834.

[33] F. Giuliani, M. Martinelli, A. Cocchi, D. Arbia, L. Fantetti, G. Roncucci, *Antimicrob. Agents Chemother.* **2010**, *54*, 637–642.

[34] D. Vecchio, T. Dai, L. Huang, L. Fantetti, G. Roncucci, M. R. Hamblin, *J. Biophotonics* **2013**, *6*, 733–742.

[35] O. Simonetti, O. Cirioni, F. Orlando, C. Alongi, G. Lucarini, C. Silvestri, A. Zizzi, L. Fantetti, G. Roncucci, A. Giacometti, A. Offidani, M. Provinciali, *Br. J. Dermatol.* **2011**, *164*, 987–995.

[36] A. Segalla, C. D. Borsarelli, S. E. Braslavsky, J. D. Spikes, G. Roncucci, D. Dei, G. Chiti, G. Jori, E. Reddi, *Photochem. Photobiol. Sci.* **2002**, *1*, 641–648.

[37] M. Li, B. Mai, A. Wang, Y. Gao, X. Wang, X. Liu, S. Song, Q. Liu, S. Wei, P. Wang, *RSC Adv.* **2017**, *7*, 40734–40744.

[38] Y. Gao, B. Mai, A. Wang, M. Li, X. Wang, K. Zhang, Q. Liu, S. Wei, P. Wang, *Photodiagnosis Photodyn. Ther.* **2018**, *21*, 316–326.

[39] V. Kussovski, V. Mantareva, I. Angelov, P. Orozova, D. Wöhrle, G. Schnurpfeil, E. Borisova, L. Avramov, *FEMS Microbiol. Lett.* **2009**, *294*, 133–140.

[40] R. T. Aroso, J. M. F. Calvete, B. Pucelik, G. Dubin, L. G. Arnaut, M. M. Pereira, J. M. Dąbrowski, *Eur. J. Med. Chem.* **2019**, *184*, 111740.

[41] V. Mantareva, C. Gol, V. Kussovski, M. Durmuş, I. Angelov, *Z. Naturforsch. C* **2019**, *74*, 183–191.

[42] Y. Zhang, K. Zheng, Z. Chen, J. Chen, P. Hu, L. Cai, Z. Iqbal, M. Huang, *Appl. Microbiol. Biotechnol.* **2017**, *101*, 4691–4700.

[43] D. M. G. C. Rocha, N. Venkatramaiah, M. C. Gomes, A. Almeida, M. A. F. Faustino, F. A. Almeida Paz, Â. Cunha, J. P. C. Tomé, *Photochem. Photobiol. Sci.* **2015**, *14*, 1872–1879.

[44] L. M. O. Lourenço, A. Sousa, M. C. Gomes, M. A. F. Faustino, A. Almeida, A. M. S. Silva, M. G. P. M. S. Neves, J. A. S. Cavaleiro, Â. Cunha, J. P. C. Tomé, *Photochem. Photobiol. Sci.* **2015**, *14*, 1853–1863.

[45] J. B. Pereira, E. F. A. Carvalho, M. A. F. Faustino, R. Fernandes, M. G. P. M. S. Neves, J. A. S. Cavaleiro, N. C. M. Gomes, Â. Cunha, A. Almeida, J. P. C. Tomé, *Photochem. Photobiol.* **2012**, *88*, 537–547.

[46] L. M. O. Lourenço, D. M. G. C. Rocha, C. I. V. Ramos, M. C. Gomes, A. Almeida, M. A. F. Faustino, F. A. Almeida Paz, M. G. P. M. S. Neves, Â. Cunha, J. P. C. Tomé, *ChemPhotoChem* **2019**, *3*, 251–260.

[47] M. B. Spesia, M. Rovera, E. N. Durantini, *Eur. J. Med. Chem.* **2010**, *45*, 2198–2205.

[48] V. Mantareva, V. Kussovski, I. Angelov, E. Borisova, L. Avramov, G. Schnurpfeil, D. Wöhrle, *Bioorg. Med. Chem.* **2007**, *15*, 4829–4835.

[49] A. Minnock, D. I. Vernon, J. Schofield, J. Griffiths, J. Howard Parish, S. B. Brown, *J. Photochem. Photobiol. B* **1996**, *32*, 159–164.

[50] Ü. İşci, M. Beyreis, N. Tortik, S. Z. Topal, M. Glueck, V. Ahsen, F. Dumoulin, T. Kiesslich, K. Plaetzer, *Photodiagn. Photodyn. Ther.* **2016**, *13*, 40–47.

[51] M. G. Strakhovskaya, Y. N. Antonenko, A. A. Pashkovskaya, E. A. Kotova, V. Kireev, V. G. Zhukhovitsky, N. A. Kuznetsova, O. A. Yuzhakova, V. M. Negrimovsky, A. B. Rubin, *Biochem.* **2009**, *74*, 1305–1314.

[52] V. N. Nemykin, S. V. Dudkin, F. Dumoulin, C. Hirel, A. G. Gürek, V. Ahsen, *Arkivoc* **2014**, 142–204.

[53] A. Galstyan, U. Dobrindt, *J. Mater. Chem. B* **2018**, *6*, 4630–4637.

[54] X. Li, D. Lee, J. D. Huang, J. Yoon, *Angew. Chem. Int. Ed.* **2018**, *57*, 9885–9890; *Angew. Chem.* **2018**, *130*, 10033–10038.

[55] A. Galstyan, A. Ricker, H. Nüsse, J. Klingauf, U. Dobrindt, *ACS Appl. Bio Mater.* **2020**, *3*, 400–411.

[56] E. Lee, X. Li, J. Oh, N. Kwon, G. Kim, D. Kim, J. Yoon, *Chem. Sci.* **2020**, *11*, 5735–5739 .

[57] Z. Chen, S. Zhou, J. Chen, L. Li, P. Hu, S. Chen, M. Huang, *J. Lumin.* **2014**, *152*, 103–107.

[58] Z. Chen, Y. Zhang, D. Wang, L. Li, S. Zhou, J. H. Huang, J. Chen, P. Hu, M. Huang, *J. Biomed. Opt.* **2016**, *21*, 018001.

[59] M. Á. Revuelta-Maza, P. González-Jiménez, C. Hally, M. Agut, S. Nonell, G. de la Torre, T. Torres, *Eur. J. Med. Chem.* **2020**, *187*, 111957.

[60] M. Wilson, J. Pratten, *Lasers Surg. Med.* **1995**, *16*, 272–276.

[61] M. Griffiths, *J. Antimicrob. Chemother.* **1997**, *40*, 873–876.

[62] R. Ruiz-González, F. Setaro, Ò. Gulías, M. Agut, U. Hahn, T. Torres, S. Nonell, *Org. Biomol. Chem.* **2017**, *15*, 9008–9017.

[63] N. Saki, M. Akin, A. Atsay, H. R. Pekbelgin Karaoglu, M. B. Kocak, *Inorg. Chem. Commun.* **2018**, *95*, 122–129.

[64] V. N. Mantareva, I. Angelov, D. Wöhrle, E. Borisova, V. Kussovski, *J. Porphyr. Phthalocyanines* **2013**, *17*, 399–416.

[65] V. Mantareva, V. Kussovski, I. Angelov, D. Wöhrle, R. Dimitrov, E. Popova, S. Dimitrov, *Photochem. Photobiol. Sci.* **2011**, *10*, 91–102.

[66] V. Mantareva, I. Angelov, V. Kussovski, R. Dimitrov, L. Lapok, D. Wöhrle, *Eur. J. Med. Chem.* **2011**, *46*, 4430–4440.

[67] V. Kussovski, V. Mantareva, I. Angelov, L. Avramov, E. Popova, S. Dimitrov, in *Biophotonics Photonic Solut. Better Heal. Care III* (Eds.: J. Popp, W. Drexler, V. V. Tuchin, D. L. Matthews), **2012**, p.84273X.

[68] J. Dlugaszewska, W. Szczolko, T. Koczorowski, P. Skupin-Mrugalska, A. Teubert, K. Konopka, M. Kucinska, M. Murias, N. Düzgüneş, J. Mielcarek, T. Goslinski, *J. Inorg. Biochem.* **2017**, *172*, 67–79.

[69] Y. Shisaka, Y. Iwai, S. Yamada, H. Uehara, T. Tosha, H. Sugimoto, Y. Shiro, J. K. Stanfield, K. Ogawa, Y. Watanabe, O. Shoji, *ACS Chem. Biol.* **2019**, *14*, 1637–1642.

[70] R. Yin, T. Agrawal, U. Khan, G. K. Gupta, V. Rai, Y.-Y. Huang, M. R. Hamblin, *Nanomedicine* **2015**, *10*, 2379–2404.

[71] *Vesicles and Micelles, W. C. de Vries, B. J. Ravoo, in Supramolecular Chemistry in Water* (Ed.: S. Kubik), Wiley-VCH, Weinheim, **2019**, pp. 375–411.

[72] S. Pottanam Chali, B. J. Ravoo, *Angew. Chem. Int. Ed.* **2020**, *59*, 2962–2972; *Angew. Chem.* **2020**, *132*, 2982–2993.

[73] M. Miretti, L. Juri, M. C. Cosiansi, T. C. Tempesti, M. T. Baumgartner, *ChemistrySelect* **2019**, *4*, 9726–9730.

[74] J. P. F. Longo, S. C. Leal, A. R. Simioni, M. de Fátima Menezes Almeida-Santos, A. C. Tedesco, R. B. Azevedo, *Lasers Med. Sci.* **2012**, *27*, 575–584.

[75] A. P. D. Ribeiro, M. C. Andrade, V. S. Bagnato, C. E. Vergani, F. L. Primo, A. C. Tedesco, A. C. Pavarina, *Lasers Med. Sci.* **2015**, *30*, 549–559.

[76] A. Galstyan, U. Kauscher, D. Block, B. J. B. J. Ravoo, C. A. C. A. Strassert, *ACS Appl. Mater. Interfaces* **2016**, *8*, 12631–12637.

[77] E. Anaya-Plaza, E. van de Winckel, J. Mikkilä, J.-M. Malho, O. Ikkala, O. Gulías, R. Bresolí-Obach, M. Agut, S. Nonell, T. Torres, M. A. Kostiainen, A. de la Escosura, *Chem. Eur. J.* **2017**, *23*, 4320–4326.

[78] R. Bonnett, M. A. Krysteva, I. G. Lalov, S. V. Artarsky, *Water Res.* **2006**, *40*, 1269–1275.

[79] F. Bayat, A. R. Karimi, *Int. J. Biol. Macromol.* **2019**, *129*, 927–935.

[80] J. Chen, W. Wang, P. Hu, D. Wang, F. Lin, J. Xue, Z. Chen, Z. Iqbal, M. Huang, *Dye. Pigment.* **2017**, *140*, 236–243.

[81] W. Tong, Y. Xiong, S. Duan, X. Ding, F.-J. Xu, *Biomater. Sci.* **2019**, *7*, 1905–1918.

[82] N. E. Grammatikova, L. George, Z. Ahmed, N. R. Candeias, N. A. Durandin, A. Efimov, *J. Mater. Chem. B* **2019**, *7*, 4379–4384.

[83] K. Strokov, A. H. Schäfer, U. Dobrindt, A. Galstyan, *ACS Appl. Bio Mater.* **2020**, *3*, 3751–3760.

[84] J. Dolanský, P. Henke, P. Kubát, A. Fraix, S. Sortino, J. Mosinger, *ACS Appl. Mater. Interfaces* **2015**, *7*, 22980–22989.

[85] J. Sun, S. Kormakov, Y. Liu, Y. Huang, D. Wu, Z. Yang, *Molecules* **2018**, *23*, 1704.

[86] N. Masilela, E. Antunes, T. Nyokong, *J. Porphyr. Phthalocyanines* **2013**, *17*, 417–430.

[87] T. Mthethwa, T. Nyokong, *Photochem. Photobiol. Sci.* **2015**, *14*, 1346–1356.

[88] N. Rapulenyane, E. Antunes, T. Nyokong, *New J. Chem.* **2013**, *37*, 1216.

[89] N. Masilela, T. Nyokong, *J. Photochem. Photobiol. A* **2013**, *255*, 1–9.

[90] D. M. Mafukidze, A. Sindelo, T. Nyokong, *Spectrochim. Acta Part A* **2019**, *219*, 333–345.

[91] N. Nombona, E. Antunes, W. Chidawanyika, P. Kleyi, Z. Tshentu, T. Nyokong, *J. Photochem. Photobiol. A* **2012**, *233*, 24–33.

[92] G. G. Matlou, T. Nyokong, *Dye Pigment.* **2020**, *176*, 108237.

[93] O. L. Osifeko, I. Uddin, P. N. Mashazi, T. Nyokong, *New J. Chem.* **2016**, *40*, 2710–2721.

[94] a) K. Albert, H.-Y. Hsu, *Molecules* **2016**, *21*, 1585; b) N. Panwar, A. M. Soehartono, K. K. Chan, S. Zeng, G. Xu, J. Qu, P. Coquet, K.-T. Yong, X. Chen, *Chem. Rev.* **2019**, *119*, 9559–9656; c) K. Yang, L. Feng, X. Shi, Z. Liu, *Chem. Soc. Rev.* **2013**, *42*, 530–547.

[95] Y. I. Openda, P. Sen, M. Managa, T. Nyokong, *Photodiagnosis Photodyn. Ther.* **2020**, *29*, 101607.

[96] N. M. Das, A. K. Singh, D. Ghosh, D. Bandyopadhyay, *Nanoscale Adv.* **2019**, *1*, 3727–3740.

[97] X. Zhou, Z. Chen, Y. Wang, Y. Guo, C.-H. Tung, F. Zhang, X. Liu, *Chem. Commun.* **2013**, *49*, 10614.

[98] X. Chen, S. Wu, D. Ma, J. Chen, Q. Guo, X. Han, K. Chen, H. Yang, Y. Huang, Y. Peng, *Chem. Commun.* **2018**, *54*, 13279–13282.

[99] Y. Gerasymchuk, A. Lukowiak, A. Wedzynska, A. Kedziora, G. Bugla-Ploskonska, D. Piatek, T. Bachanek, V. Chernii, L. Tomachynski, W. Strek, *J. Inorg. Biochem.* **2016**, *159*, 142–148.

[100] C. A. Strassert, M. Otter, R. Q. Albuquerque, A. Höne, Y. Vida, B. Maier, L. De Cola, *Angew. Chem. Int. Ed.* **2009**, *48*, 7928–7931; *Angew. Chem.* **2009**, *121*, 8070–8073.

[101] M. Grüner, L. Tuchscherr, B. Löffler, D. Gonnissen, K. Riehemann, M. C. Staniford, U. Kynast, C. A. Strassert, *ACS Appl. Mater. Interfaces* **2015**, *7*, 20965–20971.

[102] S. Li, S. Cui, D. Yin, Q. Zhu, Y. Ma, Z. Qian, Y. Gu, *Nanoscale* **2017**, *9*, 3912–3924.

[103] M. C. Grüner, M. S. Arai, M. Carreira, N. Inada, A. S. S. de Camargo, *ACS Appl. Bio Mater.* **2018**, *1*, 1028–1036.

[104] L. Fernández, Z. Lin, R. J. Schneider, V. I. Esteves, Â. Cunha, J. P. C. Tomé, *ChemPhotoChem* **2018**, *2*, 596–605.